

CD163 receptor editing for resistance to porcine reproductive and respiratory syndrome virus  
(PRRSV)

by

Ana Maria Mihaela Stoian

B.S., University of Bucharest, 2013  
M.S., University of Bucharest, 2015

AN ABSTRACT OF A DISSERTATION

submitted in partial fulfillment of the requirements for the degree

DOCTOR OF PHILOSOPHY

Department of Diagnostic Medicine and Pathobiology  
College of Veterinary Medicine

KANSAS STATE UNIVERSITY  
Manhattan, Kansas

2020

## Abstract

Porcine reproductive and respiratory syndrome virus (PRRSV) is one of the most economically destructive viruses affecting swine worldwide. In the U.S. alone, annual estimates indicate losses to national swine herds of \$664 million. PRRSV isolates can be divided into two different genotypes, PRRSV-1 or PRRSV-2, which share only about 70% identity at the nucleotide level. Previous work showed that pigs lacking CD163 expression on macrophages are protected from PRRSV-2 infection (Whitworth et al., 2016). This receptor is composed of nine scavenger receptor cysteine-rich (SRCR) domains and two proline-serine-threonine (PST)-rich regions, one between SRCR6 and SRCR7, and one between SRCR9 and the transmembrane region and cytoplasmic tail.

The purpose of the first study was to identify domains in CD163 that are necessary for infection with a PRRSV-2 isolate. The model system consisted of transfecting HEK cells with plasmids that expressed various CD163 domain deletions and an enhanced green fluorescent protein (EGFP) tag. After two days, the cells were infected with a P129 isolate expressing red fluorescent protein (RFP). The results showed that transfected cells possessing a deletion of the 101 amino acid SRCR5 or disruption of any of the conserved disulfide bonds within SRCR5 of CD163 were resistant to infection. Deletion of the 16 amino acid PSTII domain also has a negative impact on infection. The importance of both SRCR5 and PSTII domains in PRRSV infection indicates that the viral protein complex on the surface of the virion may form multiple contacts with CD163.

A recent study showed that CD163 pigs containing a SRCR5 domain swap with the corresponding homolog SRCR8 from the hCD163L1 protein became resistant to PRRSV-1 but not PRRSV-2 (Well et al., 2017), showing that the viruses recognize different peptide sequences

within SRCR5. An analysis of various studies that demonstrated the requirement of SRCR5 for PRRSV infection showed that some SRCR5 deletion constructs retained the ability to sustain a low-level of infection when retaining the SRCR4/5 inter-domain region, AHRK. Thus, the purpose of the second study was to identify the minimum changes in SRCR5 and the SRCR4/5 interdomain region sufficient to make HEK cells resistant to infection with both PRRSV genotypes. The results from this study showed that the insertion of proline-arginine (PR) after amino acids 57 and 99 inhibits infection with a PRRSV-1 isolate, whereas PR insertion after amino acids 8, 47, 54 and 99, inhibits PRRSV-2 infection. Furthermore, the deletion of the SRCR4/5 interdomain sequence, AHRK, also blocks infection.

A monoclonal antibody (mAb) 2A10 was previously produced by immunizing pigs with porcine alveolar macrophages and has been used in various CD163-related experiments. There is currently no information regarding the location of the epitope recognized by this antibody, therefore, the goal of the last study was to determine this. By western blot analysis, immunofluorescence antibody assay and flow cytometry, we identified SRCR1 as the region recognized by the mAb 2A10.

The data presented in this dissertation provided valuable tools for refinement of *in vitro* receptor editing approaches for prevention of PRRSV or other swine diseases.

CD163 receptor editing for resistance to porcine reproductive and respiratory syndrome virus  
(PRRSV)

by

Ana Maria Mihaela Stoian

B.S., University of Bucharest, 2013  
M.S., University of Bucharest, 2015

A DISSERTATION

submitted in partial fulfillment of the requirements for the degree

DOCTOR OF PHILOSOPHY

Department of Diagnostic Medicine and Pathobiology  
College of Veterinary Medicine

KANSAS STATE UNIVERSITY  
Manhattan, Kansas

2020

Approved by:

Co-Major Professor  
Raymond R. R. Rowland

Approved by:

Co-Major Professor  
Megan C. Niederwerder

# **Copyright**

© Ana Maria Mihaela Stoian 2020

## Abstract

Porcine reproductive and respiratory syndrome virus (PRRSV) is one of the most economically destructive viruses affecting swine worldwide. In the U.S. alone, annual estimates indicate losses to national swine herds of \$664 million. PRRSV isolates can be divided into two different genotypes, PRRSV-1 or PRRSV-2, which share only about 70% identity at the nucleotide level. Previous work showed that pigs lacking CD163 expression on macrophages are protected from PRRSV-2 infection (Whitworth et al., 2016). This receptor is composed of nine scavenger receptor cysteine-rich (SRCR) domains and two proline-serine-threonine (PST)-rich regions, one between SRCR6 and SRCR7, and one between SRCR9 and the transmembrane region and cytoplasmic tail.

The purpose of the first study was to identify domains in CD163 that are necessary for infection with a PRRSV-2 isolate. The model system consisted of transfecting HEK cells with plasmids that expressed various CD163 domain deletions and an enhanced green fluorescent protein (EGFP) tag. After two days, the cells were infected with a P129 isolate expressing red fluorescent protein (RFP). The results showed that transfected cells possessing a deletion of the 101 amino acid SRCR5 or disruption of any of the conserved disulfide bonds within SRCR5 of CD163 were resistant to infection. Deletion of the 16 amino acid PSTII domain also has a negative impact on infection. The importance of both SRCR5 and PSTII domains in PRRSV infection indicates that the viral protein complex on the surface of the virion may form multiple contacts with CD163.

A recent study showed that CD163 pigs containing a SRCR5 domain swap with the corresponding homolog SRCR8 from the hCD163L1 protein became resistant to PRRSV-1 but not PRRSV-2 (Well et al., 2017), showing that the viruses recognize different peptide sequences

within SRCR5. An analysis of various studies that demonstrated the requirement of SRCR5 for PRRSV infection showed that some SRCR5 deletion constructs retained the ability to sustain a low-level of infection when retaining the SRCR4/5 inter-domain region, AHRK. Thus, the purpose of the second study was to identify the minimum changes in SRCR5 and the SRCR4/5 interdomain region sufficient to make HEK cells resistant to infection with both PRRSV genotypes. The results from this study showed that the insertion of proline-arginine (PR) after amino acids 57 and 99 inhibits infection with a PRRSV-1 isolate, whereas PR insertion after amino acids 8, 47, 54 and 99, inhibits PRRSV-2 infection. Furthermore, the deletion of the SRCR4/5 interdomain sequence, AHRK, also blocks infection.

A monoclonal antibody (mAb) 2A10 was previously produced by immunizing pigs with porcine alveolar macrophages and has been used in various CD163-related experiments. There is currently no information regarding the location of the epitope recognized by this antibody, therefore, the goal of the last study was to determine this. By western blot analysis, immunofluorescence antibody assay and flow cytometry, we identified SRCR1 as the region recognized by the mAb 2A10.

The data presented in this dissertation provided valuable tools for refinement of *in vitro* receptor editing approaches for prevention of PRRSV or other swine diseases.

# Table of Contents

List of Figures .....	x
List of Tables .....	xv
Acknowledgements .....	xvi
Dedication.....	xvii
Chapter 1 - Challenges for Porcine Reproductive and Respiratory Syndrome (PRRS) Vaccine	
Design: Reviewing Virus Glycoprotein Interactions with CD163 and Targets of Virus	
Neutralization.....	1
INTRODUCTION .....	1
CD163 as the sole receptor for PRRSV .....	4
The interaction between pCD163 and PRRSV glycoproteins .....	7
PRRSV neutralization and escape from homologous and broadly neutralizing activity through the GP5/M heterodimer .....	10
SUMMARY .....	14
ACKNOWLEDGEMENTS.....	16
Chapter 2 - Receptor editing approaches for domains and regions of CD163 that are involved in infection with a porcine reproductive and respiratory syndrome virus-2 (PRRSV-2).....	21
INTRODUCTION .....	21
MATERIALS AND METHODS.....	22
RESULTS .....	27
SUMMARY AND CONCLUSIONS .....	29
Chapter 3 - Peptide sequences in scavenger receptor cysteine rich (SRCR) protein domain 5 of porcine CD163 involved in infection with a porcine reproductive and respiratory syndrome virus (PRRSV) .....	38
INTRODUCTION .....	38
MATERIALS AND METHODS.....	39
RESULTS .....	44
SUMMARY AND CONCLUSIONS .....	48
Chapter 4 - Characterization of monoclonal antibody 2A10 against different porcine CD163 deletion constructs.....	64

INTRODUCTION .....	64
MATERIALS AND METHODS.....	64
RESULTS .....	69
SUMMARY AND CONCLUSIONS .....	71
Chapter 5 - Final remarks .....	77
ACKNOWLEDGEMENTS.....	80
REFERENCES .....	81

## List of Figures

- Figure 1.1. Representation of porcine reproductive and respiratory syndrome virus-2 (PRRSV-2) virion surface proteins. The proteins are shown for a representative PRRSV-2 isolate. The minor glycoproteins GP2–4 form a heterotrimer protruding from the virion surface. The surface is dominated by GP5-M heterodimers. The M protein is unglycosylated. The position of the glycosylation sites (circles) for GP2–5 are from Das et al. (2011) and Ansari et al. (2006). Asterisks show those N-sites required for infection (Das et al., 2011; Ansari et al., 2006). The dashed line identifies the disulfide bond between GP5 and M. The structures are not drawn to scale. ....17
- Figure 1.2. Porcine CD163 organization and SRCR5 peptide sequence. This illustration shows the location of the different domains in porcine CD163 (pCD163). The shaded regions are domains that participate in PRRSV infection of cDNA transfected human embryonic kidney (HEK) cells (Van Gorp et al., 2010). The peptide sequences show a comparison between SRCR5 of pCD163 and SRCR8 from the human CD163-like protein (Wells et al., 2017). The asterisk shows the location of the R561A mutation described in Ma et al. (2017). .....18
- Figure 1.3. Functional domains in PRRSV GP4. The locations of the N-glycosylation sites are shown for PRRSV-2 (PRRSV-1 in parentheses). The neutralizing epitope—GP4(56–68)—is described in Vanhee et al. (2010). Asterisks show amino acids shared by PRRSV-1 and PRRSV-2. The GPI anchor for PRRSV-2 and the proposed CD163 binding domains are described in Du et al. (2012) and Chen et al. (2018), respectively. The illustration is based on GP4 from representative PRRSV-1 Lelystad (LV) and PRRSV-2 VR-2332 (VR), GenBank M96262.2 and U87392.3, respectively. ....19
- Figure 1.4. Effect of mutations in GP5 and M proteins on the orientation of a conserved linear epitope. Amino acid mutations (shown in red) influence the orientation of a conserved linear neutralizing epitope. The mutations are sufficient to block neutralizing antibody without affecting how the oligopeptide functions in its interaction with the host cell. N-glycosylation sites provide further shielding. The right-hand figure shows the location of the N-glycosylation sites (circles) and putative neutralizing epitope (dashed lines) for representative PRRS viruses and for lactate dehydrogenase-elevating virus (LDV). .....20

Figure 2.1. CD163 constructs used to identify domains involved in PRRSV-2 infection. (A) Deletion mutants used in the transfection of HEK cells. Ovals and squares identify the SRCR and PST domains, respectively. (B) Result for PRRSV infection of transfected HEK cells. Key: (+++), similar to results for wild-type CD163 including numerous large clusters of infected cells; (++) , several small clusters of infected cells; (+), multiple single infected cells, but no clusters; (+/-), a few scattered infected cells; (-), no detectable infected cells. (C) Results for western blots using anti-GFP antibody for the detection of the CD163-EGFP fusion proteins. ....33

Figure 2.2. Co-localization of CD163-EGFP and P129-RFP in HEK cells. Non-permissive HEK cells were transfected with different CD163 deletion constructs (represented in green). At 24-48 hrs post-transfection, the cells were infected with P129-RFP (represented in red). A positive result for infection is recorded as a cell expressing both green and red fluorescence. ....34

Figure 2.3. Surface expression of CD163 constructs expressed in transfected HEK cells. Letters refer to the constructs shown in Figure 2.1A. The top row of histograms are cells stained with a rabbit anti-CD163 antibody prepared against an oligopeptide in SRCR9 (Biorbyt). The bottom histograms show cells stained with a mouse mAb 2A10 (BIO-RAD). The GFP expression is represented in green, the mAb 2A10 staining in red and the isotype control in gray. Cells were stained 48 hrs after transfection. The CD163 staining results are shown as percentage of CD163-positive cells from the GFP-positive gated population. ....35

Figure 2.4. Effect of cysteine to alanine substitutions in SRCR5 on PRRSV infection. (A) Disulfide bonds in SRCR5 were removed by making cysteine to alanine substitutions at C1, C3, C5 or C7. The locations of the different disulfide bonds are according to Ma et al. (2016). The number above each cysteine is the location within the SRCR5 peptide sequence. The number in parentheses is the fraction of infected cells compared to the wild-type CD163 as the positive control. All infections were performed on the same 24-well plate. The percent of green cells infected for the wild-type CD163 was 61.2%. The locations of the 41 amino acid deletion described by Guo et al. (2019) and ligand binding pocket (LBP; bold underlined letters) are identified in the SRCR5 peptide sequence. (B) shows the surface expression of CD163 for the cysteine to alanine mutated constructs. The GFP expression is represented in green, the mAb 2A10 staining in red and the isotype control in

gray. Cells were stained 48 hrs after transfection. The mAb 2A10 staining results are shown as percentage of CD163-positive cells from the GFP-positive gated population. ....36

Figure 2.5. Infection of HEK cells expressing CD163 PSTII constructs. (A) shows the peptide sequence for the PSTII region covered by Exons 12, 13 and 14. The letters in bold show the amino acid of the PSTII domain. (B) is a diagram of the PSTII constructs used for transfection of HEK cells. The shaded box shows the location of the substitution of the GRSS peptide sequence with three alanine residues. The key for infection is the same as described in Figure 2.1. (C) shows the surface expression of CD163 for the PSTII constructs. The GFP expression is represented in green, the mAb 2A10 staining in red and the isotype control in gray. Cells were stained 48 hrs after transfection. The mAb 2A10 staining results are shown as percentage of CD163-positive cells from the GFP-positive gated population. ....37

Figure 3.1. Surface expression of CD163 interdomain constructs expressed in transfected HEK cells. Letters refer to the constructs shown in Table 3.2. Surface expression of CD163 constructs expressed in HEK cells. The histograms show the GFP expression green, the mAb 2A10 staining in red and the isotype control in gray. Cells were stained 48 hrs after transfection. The mAb 2A10 staining results are shown as percentage of CD163-positive cells from the GFP-positive gated population.....56

Figure 3.2. Location and effect of PR insertions in SRCR5 on PRRSV-2 infection. (A) The SRCR5 peptide sequence is from GenBank No. EU016226. The arrows show the location and direction of beta strands and the dotted lines, the location of alpha helices. The asterisks show the location of the proline-arginine insertions. Below each construct is the result for infection of transfected HEK cells. (B) Additional PR substitutions in the vicinity of PR-55. Key: (+++), similar to results for wild-type CD163 including numerous large clusters of infected cells; (++) , several small clusters of infected cells; (+), multiple single infected cells, but no clusters; (+/-), a few scattered infected cells; (-), no detectable infected cells. 57

Figure 3.3. Surface expression of SRCR5 PR insertion constructs expressed in HEK cells. The histograms show the GFP expression green, the mAb 2A10 staining in red and the isotype control in gray. Cells were stained 48 hrs after transfection. The mAb 2A10 staining results are shown as percentage of CD163-positive cells from the GFP-positive gated population.58

Figure 3.4. Growth curves for HEK293T cells transfected with wild-type and mutant CD163 constructs. HEK cells transfected with different mutant constructs and after 24 hrs infected with PRRSV P129-RFP. Two hours post-infection, the cells were washed, and media was collected every 12 hrs. The TCID<sub>50</sub> was calculated by titration of viruses on MARC-145 cells. Results are shown for a single experiment. ....59

Figure 3.5. Effect of Glu to Lys substitution at position 58 (E58K) of SRCR5. (A) Non-permissive HEK cells were transfected with either E58K mutation or WT CD163 (represented in green). At 24-48 hrs post-transfection, the cells were infected with PRRSV-1 at a MOI of 0.1 and with PRRSV-2 with a MOI of 1. Following staining against the PRRSV N-protein (represented in red), a positive result for infection was recorded as a cell expressing both green and red fluorescence. (B) The infection on HEK cells transfected with the E58K mutation was measured as percent of PRRSV positive cells. Data represents means from three independent experiments. A  $p < 0.05$  indicates significantly reduced level of infection for PRRSV-1. ....60

Figure 3.6. Predicted location and of PR insertions in SRCR5. Each amino acid pair in the ribbon structure identifies the location of each PR insertion. The structures are based on the X-ray crystallography data deposited in RCSB Protein Data Bank (PDB code 5JFB) and viewed using UCSF Chimera (Pettersen et al., 2004). The key for the infection rate for each mutation is described in Figure 3.2. ....61

Figure 3.7. Surface location of mutations in SRCR5 that affect PRRSV-1 and PRRSV-2 infection. The figure is a surface model showing the location of the PR insertions in color. Each colored region represents the same dipeptides shown in Figure 3.2. Orientation A shows all mutation sites. Orientation B shows a 180° rotation of the polypeptide. ....62

Figure 3.8. Predicted effects of PR insertions on the secondary structure of SRCR5. The ribbon model structures were computer-generated using the same modeling software described in Figure 3.6. The mutation name and C-value are shown for each structure. Red shows the location for each insertion and the green represents the PR dipeptide. The wild-type structure is in the middle. ....63

Figure 4.1. CD163 constructs used to characterize the CD163 mAb 2A10. (A) Deletion mutants used in the transfection of HEK cells. Ovals and squares identify the SRCR and PST domains, respectively. (B) Result for western blot using anti-GFP antibody for the detection

of the CD163-EGFP fusion protein. (C) Results for western blot using the anti-CD163 mAb 2A10. ....73

Figure 4.2. Detection of CD163 expression in transfected HEK cells by immunofluorescence antibody assay using the mAb 2A10. HEK cells were transfected with different CD163 deletion constructs and after 48 hrs were visualized under the fluorescence microscope for GFP expression (green); the transfected cells were fixed and incubated with a CD163 specific mAb (2A10 clone), followed by an incubation with Alexa Fluor 594-conjugated goat anti-mouse IgG secondary antibody (red). Cells were counterstained with DAPI (blue). ....74

Figure 4.3. Surface expression of CD163 deletion constructs expressed in HEK cells. The histograms show the GFP expression green, the mAb 2A10 staining in red and the isotype control in gray. Cells were stained 48 hrs after transfection. The mAb 2A10 staining results are shown as percentage of CD163-positive cells from the GFP-positive gated population.75

Figure 4.4. Production of CD163 SRCR1 domain. (A) SDS-PAGE of His-tagged SRCR1 recombinant protein preparation, followed by Coomassie blue staining. (B) Western blot analysis using anti-His tag mAb. (C) Western blot analysis using anti-CD163 mAb (2A10 clone). For all panels, the left lane shows the molecular weight marker. ....76

## List of Tables

Table 2.1. Primers for amplification of CD163 constructs shown in Figure 2.1. The underlined nucleotides identify restriction sites; in italics is represented the nucleotide that was added after the PacI site to ensure an in-frame construct. ....	32
Table 3.1. Primers for amplification of CD163 inter-domain constructs shown in Table 3.2. The underlined nucleotides identify restriction sites.....	50
Table 3.2. Peptide sequence modifications in the SRCR4/5 that affect infection. ....	51
Table 3.3. Primer sequences for the preparation of SRCR5 mutations. SacII restriction sites are underlined. ....	52
Table 3.4. Percent infection of HEK293T cells transfected with different PR dipeptide insertion constructs*. ....	53
Table 3.5. Comparison of infection results for PRRSV-1 and PRRSV-2*.....	54
Table 3.6. Effect of PR insertions on secondary structure of SRCR5*. ....	55
Table 4.1. Primers for amplification of CD163 deletion constructs shown in Figure 4.1. The underlined nucleotides identify restriction sites.....	72

## **Acknowledgements**

First, I wish to express my gratitude to my co-major professor, Dr. Bob Rowland, for his mentorship, and for the numerous opportunities that helped me develop my research and writing skills. Additionally, I would like to thank my committee members, including Dr. Megan Niederwerder (co-major professor), Dr. Ying Fang, Dr. Sally Davis, Dr. Natasha Gaudreault, Dr. Jennifer Bormann for their valuable advice during these past years. I would also like to extend my appreciation to my committee chair, Dr. Tom Platt, for his support.

Sincere gratitude to all the past and present members of the Rowland lab – Vlad Petrovan, Luca Popescu, Matthew Olcha, Laura Constance, Maureen Sheahan – for their constant laboratory research guidance. I would also like to thank Francine Rowland and Muthu Chengappa for their emotional support during difficult times.

Finally, I would like to express my genuine appreciation to my parents, Cristina and Cornel, and my brother, Cosmin, for their unconditional love and endless support during every step of my career.

## **Dedication**

*This thesis is dedicated to my beloved grandmother, Floarea.  
Even if you might not remember me, I will always remember you!*

# **Chapter 1 - Challenges for Porcine Reproductive and Respiratory Syndrome (PRRS) Vaccine Design: Reviewing Virus Glycoprotein Interactions with CD163 and Targets of Virus Neutralization**

*Published in Veterinary Sciences*

Stoian, A.M.M., & Rowland, R.R.R. (2019). Challenges for Porcine Reproductive and Respiratory Syndrome (PRRS) Vaccine Design: Reviewing Virus Glycoprotein Interactions with CD163 and Targets of Virus Neutralization. *Veterinary sciences*, 6(1), 9. doi:10.3390/vetsci6010009.

The work displayed here is published by MDPI in the *Veterinary Sciences* journal, available online at <https://doi.org/10.3390/vetsci6010009>. The introduction of the article has been altered from when it was originally published and has not undergone peer-review.

## **INTRODUCTION**

Porcine reproductive and respiratory syndrome virus (PRRSV) was first described in the USA in 1987 as an infectious agent responsible for “mystery swine disease”. Clinical signs after infection include reproductive failure during late gestation, respiratory distress in young pigs, and poor growth performance (Keffaber, 1989). PRRSV consists of two species: PRRSV-1 isolates are of European origin while PRRSV-2 originated in North America. PRRSV-1 and PRRSV-2 share ~70% identity at the nucleotide level. In addition, each species can be further divided into several clades or substrains. PRRSV, along with the closely related mouse virus, lactate dehydrogenase-elevating virus (LDV), are part of the *Arteriviridae* family, *Variarterivirinae* subfamily (Gulyaeva et al., 2017). Recently, the two PRRSV species have been

placed in genus *Betaarterivirus*, with *Ampobartevirus* and *Eurpobartevirus* as corresponding subgenera. Subsequently, *Betaarterivirus suis* 1 species was created for the original PRRSV-1 and *Betaarterivirus suis* 2 species for the PRRSV-2, respectively. The progenitor virus for PRRSV-1 was first isolated and sequenced in The Netherlands in 1991 (Wensvoort et al., 1991) and named Lelystad virus. This was followed by the isolation of VR-2332 in North America (Collins et al., 1992, Benfield et al., 1992), perhaps through the introduction of Russian wild boar (Plagemann, 2003). A separate course of evolution in North America produced PRRSV-2. Perhaps the most remarkable aspect of PRRS virus evolution is the simultaneous emergence of PRRSV-1 and PRRSV-2, which produce similar disease signs and possess a similar epidemiology/ecology. Therefore, PRRSV is a good example of how a virus with unique biological properties is able to effectively exploit unique ecological niches created by the modern swine industry.

The PRRSV genome possesses at least ten open reading frames (ORFs) flanked by a 5' leader and 3' untranslated region followed by poly-A tail. The nonstructural proteins, encoded by ORF1a and ORF1b, possess protease, replicase and host gene modulation functions. The 3' end of the genome codes for at least eight structural proteins translated from a nested 3'-coterminal set of subgenomic mRNAs possessing a common leader, a hallmark feature of the genus and the Nidovirus order. The major structural proteins, GP5, matrix (M), and nucleocapsid (N) are encoded by ORFs 5, 6, and 7, respectively. GP5 and M generally exist as a GP5-M heterodimer; however, GP5 homodimers have been identified (Matanin et al., 2008). GP2, GP3, and GP4 are minor surface glycoproteins (GPs) derived from ORFs 2, 3, and 4, respectively. Two very small unglycosylated proteins—2b (or E) and 5a—are translated from ORF2b and ORF5a, respectively (Johnson et al., 2011; Wu et al., 2001). In 2013, Kappes et al. described the association of the

nonstructural protein, nsp2, with the virion. However, there are no published data demonstrating that anti-nsp2 antibodies possess neutralizing activity.

The topological features of the virion surface are described in Spilman et al. (2009), who performed cryo-electron microscopy followed by tomographic reconstruction of purified virions derived from MARC-145 cells infected with a PRRSV-2 isolate. The surface of the virion is smooth, reflecting the predominance of short peptide sequences formed by the ectodomains of M and GP5. A small number of protrusions rise above the surface, formed by the large ectodomains of GP2, 3, and 4. The ectodomain regions of surface proteins are illustrated in Figure 1.1.

The targets for PRRSV infection are cells of monocyte/macrophage origin. It is this interaction between the virus and macrophage that is responsible for respiratory distress and immune modulation, which are associated with the onset of the porcine respiratory disease complex (PRDC). Van Breedam et al. (2010) were the first to propose a detailed model describing how PRRSV interacts with, and then enters, the macrophage host. In this model, PRRSV infection occurs in three steps, which incorporate interactions between PRRSV and three different receptor molecules on the macrophage cell surface. The first step is the initial interaction between the PRRSV M protein and heparin sulfate (HS) (Delputte et al., 2002). Blocking or removing HS does not completely abrogate infection, suggesting that the virion–HS interaction is relatively nonspecific and is designed to bring the virion into closer proximity with the macrophage surface. The second step is a higher affinity interaction between the glycosyl residues on GP5 and sialoadhesin (Sn) on the macrophage. Support for Sn as a PRRSV receptor was initially based on the characterization of monoclonal antibodies (mAbs) prepared against macrophage antigens, which inhibited PRRSV infection. Sn was identified as the ligand for one of the mAbs. Further support for Sn comes from making PRRSV non-permissive cells

permissive for infection after transfection with a plasmid expressing a porcine Sn cDNA (Vanderheijden et al., 2003). However, the acquisition of Sn by nonpermissive cells did not result in productive infection. Therefore, the role of Sn is to bind PRRSV to the macrophage surface; nonetheless, this interaction is not sufficient for virus internalization. The third step for infection is internalization, uncoating of the virion, and the release of virus nucleic acid in the cytoplasm. This step occurs through the interaction of the virion with CD163, a PRRSV receptor first described by Calvert et al. (2007). CD163 was identified based on the screening of cDNAs from a macrophage library that rendered PRRSV permissiveness to a non-permissive cell line. As indicated in the model of Van Breedam et al. (2010), CD163 is not an attachment factor or surface receptor, but participates in the later stages of internalization and release of the viral genome into the cytoplasm.

The role of Sn as the primary PRRSV receptor protein was first called into question by Welch and Calvert (2010), who observed that the transfection of non-permissive PK-15 cells, which lack Sn, with a plasmid vector expressing a CD163 cDNA was sufficient to render cells permissive for PRRSV infection. Furthermore, pigs possessing a knockout of the SIGLEC-1 gene did not express Sn on macrophages but retained the ability to support PRRSV infection to the same level as Sn wild-type pigs (Prather et al., 2013). One explanation for how SIGLEC-1 knockout pigs can support infection is based on the presence of alternative SIGLEC proteins, such as SIGLEC-10, which can substitute for the SIGLEC-1 protein (Xie et al., 2018).

### **CD163 as the sole receptor for PRRSV**

Even though there exists a large body of work and several convincing arguments in support of multiple PRRSV proteins interacting with multiple receptors and coreceptors on

macrophages and other pig cells, the overwhelming evidence supports the hypothesis that surface expression of CD163 is necessary and sufficient to support PRRSV infection.

Porcine CD163 is a 130 kDa type I transmembrane protein and a member of the group B protein cluster within the scavenger receptor cysteine-rich superfamily (SRCR-SF). Group B proteins are involved in the regulation of cellular immune responses. Based on peptide sequence homology and structure, group B proteins can be further divided into three subgroups. The first subgroup consists of CD5, CD6, and SP $\alpha$ , which are expressed by T-cells and B-cells. The second subgroup includes WC1, CD163, CD163-L1 and SCART, which are mostly found in monocytes and macrophages. The third subgroup includes DMBT1, gp-340 and SAG, which are involved in binding pathogens (Aruffo et al., 1991; Ligtenberg et al., 2007).

The porcine CD163 gene consists of 17 exons, which code for a peptide signal sequence followed by nine SRCR domains consisting of approximately 100 amino acids in length. Each domain possesses multiple cysteines, which form several internal disulfide bonds. SRCR6 and SRCR7 domains are separated by a proline-serine-threonine (PSTI) polypeptide of 35 amino acids. A second 16 amino acid PST domain, PSTII, connects SRCR9 with the transmembrane domain, which is followed by a short cytoplasmic tail. A representation of porcine CD163 (pCD163) is shown in Figure 1.2. So far, only SRCR2, SRCR3 and SRCR5 are known to be involved in biological processes. A 13-amino-acid motif in SRCR2 can bind erythrocytes and bacteria (Fabriek et al., 2007, Fabriek et al., 2009). Hemoglobin-haptoglobin (Hb-Hp) complexes are internalized after binding to SRCR3 (Kristiansen et al., 2001). SRCR5 participates in PRRSV infection (Wells et al., 2017).

CD163 as a receptor for PRRSV was first described by Calvert et al. (2007). The results showed that the transfection of non-permissive cell lines with CD163 cDNAs of simian, human,

canine, or mouse origin is sufficient to render cells fully permissive to infection. Furthermore, Whitworth et al. (2016) showed that pigs possessing a knockout (KO) of the CD163 gene were non-permissive for infection with a PRRSV-2 isolate. For these experiments, both CD163 KO and WT pigs were comingled after infection, which allowed for the continuous exposure of the CD163 KO pigs to virus shed by the infected WT pigs. In a subsequent study, macrophages from CD163 KO pigs were shown to be resistant to infection with PRRSV-1 and PRRSV-2 (Burkard et al., 2017).

Resistance to PRRSV infection localizes to a single CD163 domain, SRCR5. The deletion of SRCR5 in human embryonic kidney (HEK) cells transfected with CD163 cDNA mutants (Van Gorp et al., 2010), or pigs lacking exon 7 in the pCD163 gene, are resistant to PRRSV-1 infection (Burkard et al., 2018). Differences between PRRSV-1 and PRRSV-2 isolates in the recognition of CD163 also localize to SRCR5. Macrophages from pigs possessing a domain swap between pCD163 SRCR5 and an SRCR8 domain homolog from the human CD163-like protein retain permissiveness to PRRSV-2 but are non-permissive to infection with PRRSV-1 strains. This difference in recognition by PRRSV-1 and PRRSV-2 is located within the 31 amino acid difference between human CD163-like SRCR8 and pCD163 SRCR5 (Figure 1.2). To date, the only available information on specific amino acid residues involved in the recognition of SRCR5 by PRRSV is found in Ma et al. (2017), who prepared six pCD163 SRCR5 variants possessing substitutions of arginine or aspartic acid residues with alanine residues, located along the SRCR5 polypeptide. A single arginine to alanine substitution at position 561 in pCD163 SRCR5 was sufficient to significantly reduce infection of transfected PK-15 cells. However, the requirement of R561 for PRRSV infection is unlikely, since the

human CD163-like SRCR8 domain possesses a naturally occurring histidine substitution at the same 561 position (Figure 1.2).

Van Gorp et al. (2010) showed that other pCD163 domains, besides SRCR5, participate in PRRSV infection. For these experiments, HEK cells were transfected with pCDNA 3.1 expression plasmids possessing deletions in pCD163 or domain swaps with the human CD163-like protein. Deletion of PSTII or SRCR 7–9 resulted in complete loss of infection. Deletion of PSTI produced a significant reduction in infection (Figure 1.2).

### **The interaction between pCD163 and PRRSV glycoproteins**

The corresponding PRRSV proteins involved in interacting with CD163 are described in Das et al. (2010). For these experiments, plasmids containing ORF2 (GP2), ORF3 (GP3), ORF4 (GP4), or ORF5 (GP5) cDNAs were transfected singly or in combination into non-permissive BHK-21 cells. High levels of PRRSV gene expression were attained by transfecting cells with an expression plasmid that placed the PRRSV glycoprotein gene under the control of a T7 RNA polymerase promoter, followed by infection of transfected cells with a vaccinia virus expressing T7 polymerase. Immunoprecipitation (IP) was performed using monospecific polyclonal serum or an antibody against flag-tagged PRRSV glycoproteins. As predicted, interactions were observed between GP2, GP3 and GP4. Interestingly, GP4 coprecipitated with GP5. BHK-21 cells were made permissive for PRRSV infection after transfection with a pCD163 cDNA plasmid. The BHK-CD163 cells were transfected with the different PRRSV GP plasmids and IP performed using an anti-CD163 antibody. Only GP2 and GP4 formed specific interactions with CD163. Together, these data confirm that GP2, 3 and 4 form a heterotrimer and that the

interaction with CD163 occurs through GP2 and 4. It is possible that GP2 and 4 form multiple interactions between different domains in CD163.

As illustrated in Figure 1.1, GP2–4 possess multiple glycosylation sites. Das et al. (2011) showed that all of the predicted N-glycosylation sites shown in Figure 1.1 are functional, but the N-sites are glycosylated with different efficiencies. Figure 1.1 also identifies those glycosylation sites on GP2, 3, 4, and 5 required for PRRSV infection. These observations are based on the infection of cells with an infectious clone possessing N-glycosylation site mutations. For example, an FL12 infections clone possessing a GP2 without the N184 glycosylation site was unable to propagate in MARC-145 cells after electroporation of the infectious clone RNA. In contrast, the removal of the N178 site had no effect on replication. For GP4, all four glycosylation sites are conserved between PRRSV-1 and PRRSV-2 viruses (Figure 1.3). However, the deletion of individual glycosylation sites in GP4 had no effect on FL12 replication. In fact, infectious clones possessing deletions in individual N-glycosylation sites showed increased virus yields compared to the parent FL12 virus. The enhancement of virus replication in GP4 mutated viruses could not be explained. For GP5, Ansari et al. (2006) identified a requirement for the N44 glycosylation site in the replication of FL12 mutant viruses.

As described above, CD163 in cells coprecipitates with GP2 and GP4. For GP2, there is no correlation between the patterns of N-glycosylation, permissiveness of cells for infection, and the ability of GP2 to interact with CD163. For example, even with the removal of the N184 glycosylation site, which blocked infection, GP2 retained the ability to interact with CD163. For GP4, the removal of N37 and N84 glycosylation sites (Figure 1.3), which flank the putative neutralization epitope, greatly reduced the interaction between GP4 and CD163, with the unglycosylated form exhibiting the greatest reduction in binding.

Additional evidence for the importance of the GP2, 3, and 4 heterotrimer in the interaction of virus with host cells is found in a large body of data supporting GP4 peptide sequence domains as targets for neutralizing antibody. Kimpston-Burkgren et al. (2017) constructed a chimeric virus composed of a PRRSV-1 SD01–08 infectious clone backbone combined with ORFs 2–4 from a PRRSV-2 isolate, FL12. The chimeric virus, called SDFL24, was replication-competent in MARC-145 cells and produced viremia following infection of pigs. Vaccination of pigs with SDFL24 followed by challenge with FL12 or SD01–08 showed significantly greater levels of protection in pigs challenged with FL12. This result demonstrates that GP2–4 are antigen sources for homologous protection. This result was supported by high levels of serum virus neutralizing activity in SDFL24 pigs against FL12, but not SD01–08.

PEPSCAN analysis of a PRRSV-1 proteome, Lelystad virus (LV), identified a reactive oligopeptide, 57-GVSAAQEKISFG-68, in GP4 from LV-infected pigs (Vanhee et al., 2010), Figure 1.3). Antibodies prepared against the oligopeptide neutralized the parent virus, LV, but not PRRSV-1 isolates possessing the GP4 oligopeptides, 57-RVTAAQGRIYTR-68, or 57-RTNTTQGKV----68 (underlined amino acids show the amino acid differences). A comparison of several PRRSV-1 isolates shows that the GP4(57–68) region forms a hypervariable domain (Vanhee et al., 2010). Presumably, the hypervariable domain is responsible for antigenic variation in the epitope and eventual escape from neutralization by antibody. Further support for the importance of GP4(57–68) is found in Costers et al. (2010), who characterized several neutralizing mAbs prepared against LV. The mAbs reacted with the same GP4(57–68) oligopeptide. Using a phage display approach to screen sera from pigs infected with the Danish PRRSV-1 isolate, 111/92, Oleksiewicz et al. (2001) identified a reactive oligopeptide that covered GP4(59–71). For PRRSV-2 isolates, the GP4(56–68) domain possesses a deletion of

three amino acids. As illustrated in Figure 1.3, the GP4(57–68) region is flanked by two N-glycosylation sites, located at N37 and N84, suggest that these flanking sugar residues shield the epitope from neutralizing antibody. Interestingly, the nucleotide sequence coding for the GP4(57–68) epitope is located within the overlapping region between ORF3 and ORF4.

Even though the GP4(56–68) peptide sequence likely forms a major neutralizing epitope, the participation of this peptide sequence in the formation of an interaction with CD163 remains unclear. Recently, Chen et al. (2018) utilized a phage display library to identify peptide sequence domains in CD163 that interact with GP4. Selection was based on the ability of phage to bind immobilized recombinant GP4 derived from a PRRSV-2 isolate. The dodecapeptide, WHEYPLVWLSGY (WHE), showed the highest affinity for GP4. The oligopeptide contains the peptide sequence HEYPLV, is similar to the sequence, HRKPRLV (underlined are the identical amino acids), located at the start of pCD163 SRCR5 polypeptide. A modeling computer program—Spring On-line—identified the GP4(23–48) polypeptide as the predicted binding site for the WHE oligopeptide.

### **PRRSV neutralization and escape from homologous and broadly neutralizing activity through the GP5/M heterodimer**

In previous work, we conducted virus neutralization (VN) assays using a panel of PRRSV-2 strains along with a single PRRSV-1 isolate, LV. The results showed that pigs could be placed into four distinct VN categories or groups (Popescu et al., 2017). Group 1 pigs possess no detectable VN activity, even after vaccination and challenge. Group 2 pigs possess only VN activity against the virus used for infection. This is the classic description of homologous VN activity. Group 3 pigs neutralize more viruses than the one used for infection, but not all viruses

in the panel. This is a good description of “heterologous” VN activity, where the breadth of neutralization extends beyond the virus used for infection. And finally, Group 4 pigs possess broad VN activity in serum, which further extends the capacity of to neutralize a broad range of PRRSV-2 isolates to include PRRSV-1 strains (Robinson et al., 2015; Tribble et al., 2015). For experimentally infected pigs, only ~1% of pigs possess broadly neutralizing activity at 42 days after infection.

We identify neutralizing epitopes for PRRSV by selecting for viruses that escape neutralization in the presence of sera possessing homologous or broadly neutralizing activity. The selection steps, described in Tribble et al. (2015), begin with a 24-well plate in which every well contains a different dilution of virus combined with a different dilution neutralizing serum. After one-hour incubation at 37 °C, the entire well contents are transferred to a 24-well plate of confluent MARC-145 cells. After four days of incubation, wells with the highest concentrations of serum resulting in cytopathic effect (CPE) are pooled. For the second step, the concentration of virus is increased by placing the pooled sample on MARC-145 cells in a T-25 culture flask in the absence of anti-PRRSV serum. After three days, the virus is harvested, and the antibody selection step repeated on a new 24-well plate. The selection process is complete when all wells show CPE. To identify amino acids changes associated with escape, ORFs 2–7 corresponding to the structural genes are sequenced and the amino acid sequence compared to the parent virus. We prepared neutralization resistant viruses that escaped neutralization by homologous and broadly neutralizing sera. The escape from homologous neutralization was mapped to mutations in a hypervariable region in GP5, called HVR-2 in Figure 1.4. A deletion of the tyrosine at position 10 of the M protein in KS62 was associated with escape from broadly neutralizing serum. The Tyr-10 deletion was next to the conserved cysteine at position 9, which forms a disulfide bond

with Cys-48 in GP5. The importance of the Tyr-10 deletion was confirmed using reverse genetics and an infectious clone to construct a recombinant virus with the same Tyr-10 deletion. The recombinant deletion virus possessed all of the neutralization properties associated with the parent virus possessing the Tyr-10 deletion. Other properties of the Tyr-10 deletion virus included escape from broadly neutralizing sera from pigs infected with other viruses while retaining sensitivity to serum possessing homologous neutralizing activity. These data show that homologous and broadly neutralizing antibodies recognize different epitopes. Moreover, we recognize that possibility that some of the antibody recognition sites may be more conformational in nature.

As illustrated in Figure 1.4, the 61 amino acid ectodomain region of PRRSV-2 GP5 contains a peptide signal sequence along with two hypervariable regions (HVRs). Mutations in HVR-1 can create additional glycosylation sites and affect the location of the peptide signal cleavage sites (Popescu et al., 2017). Two conserved N-glycosylation sites downstream of HVR-1 are located at amino acid positions 44 and 51 for PRRSV-2, 46 and 53 for PRRSV-1, and 44 and 51 for LDV. Near the two N-glycosylation sites is a region occupied by a relatively conserved linear epitope. By using a phage display approach, Ostrowski et al. (2002) identified a peptide sequence, called Epitope B, which covered amino acids 37 to 45 of GP5. The peptide sequence is found in a larger epitope characterized by Plagemann et al. (2002). In 2004, Plagemann also identified similar epitopes in GP5 of PRRSV-1 and LDV (Figure 1.4). A second, short hypervariable region, called HVR-2, is located just downstream of the N51 site (Delisle et al., 2012). The escape of a virus from homologous neutralization is typically explained by the process of antigenic variation in hypervariable regions of GP4 and GP5 (Vanhee et al., 2010; Popescu et al., 2017). Figure 1.4 presents a proposed model to explain how a conserved linear

epitope, such as the one identified in GP5, escapes neutralization by broadly neutralizing serum. A possible explanation would be that mutations in the M protein, and HVR-1 and HVR-2 of GP5 can change epitope orientation in a manner sufficient to prevent antibody accessibility without changing the conserved epitope's peptide sequence or its function.

GP5 as a principal target for neutralizing antibody, is supported by research conducted using LDV. Similar to PRRSV-1 and PRRSV-2, LDV GP5 (also known as VP3) possesses two conserved glycosylation sites along with a third site at position 35. Naturally occurring strains of LDV lacking the N35 and N45 sites show a tropism for motor neurons. The cytopathic removal of neurons results in paralysis. Interestingly, the N35/N45 deletion viruses are removed in response to the induction of a strong neutralizing antibody response by the mouse. The remaining residual viruses eventually reacquire both glycosylation sites and become persistent (Plagemann, 2001). A similar role for N-glycan shielding in GP5 of PRRSV was demonstrated using reverse genetics of an infectious PRRSV-2 cDNA clone (Ansari et al., 2006). The results showed that viruses lacking N44 were non-viable in culture, indicating a requirement of N-glycosylation for replication. The removal of the N34 and N51 glycosylation sites resulted in the increased sensitivity of recombinant viruses to neutralization by antibody from pigs infected with the parent or recombinant viruses. Faaberg et al. (2006) observed enhanced neutralization activity after infection of pigs with naturally occurring variants of VR-2332, which lacked N30/N33 in GP5. Similar to LDV, the deleted N-glycosylation sites were reacquired during infection of pigs (Vu et al., 2011). The restoration of N-glycosylation in GP5 resulted in prolonged infection and the resistance of viruses to neutralizing antibody.

## SUMMARY

Stringent biosecurity measures along with the application of effective vaccines provide the best strategy for the control and eventual elimination of PRRS. To date, modified live attenuated viruses provide the greatest levels of protection, but fall short in a variety of areas. Inactivated virus, subunit, and vectored approaches are important options, but their development is stymied by a failure to provide protective immunity. The complex nature of the PRRSV neutralization response remains a serious obstacle to vaccine development. Several neutralizing epitopes have been identified within the PRRS viral proteins. PEPSCAN analysis identified a short peptide sequence in GP4 of PRRSV-1 as a linear epitope recognized by a mAb with neutralizing activity (Meulenberg et al., 1997). Moreover, Vanhee et al. (2011) characterized additional neutralizing epitopes in GP2 and GP3 proteins of PRRSV-1. In another study done by Zhou et al. (2006), mAbs against GP3 of PRRSV-2 were used to identify neutralizing epitopes. Antigenic variation in the viral proteins provides a logical rationale for how viruses can escape homologous neutralizing antibody, but antigenic variation in these proteins fails to explain a broadly neutralizing response directed against highly conserved peptide sequences. A conserved oligopeptide in GP5 flanked by glycosylation sites and hypervariable regions presents an “ideal” broadly neutralizing epitope.

Disrupting the interaction between PRRSV and CD163 can be used as an approach for vaccine development. This review describes an apparent conundrum regarding CD163, its corresponding ligand, GP4, and the overall nature of broad virus neutralization, which appears to localize to GP5. The epitope in GP5 is consistent with a broadly neutralizing epitope; however, the molecular basis for the interaction of the peptide sequence with a corresponding receptor on the macrophage remains unclear and raises an important question: Is there an unidentified cell

receptor that interacts with the ectodomain of GP5? The preparation of a panel of mAbs possessing homologous, heterologous, and broad neutralization activities is needed to address this conundrum.

## **ACKNOWLEDGEMENTS**

The authors wish to acknowledge the editorial assistance of Maureen Sheahan and Carol Wyatt.

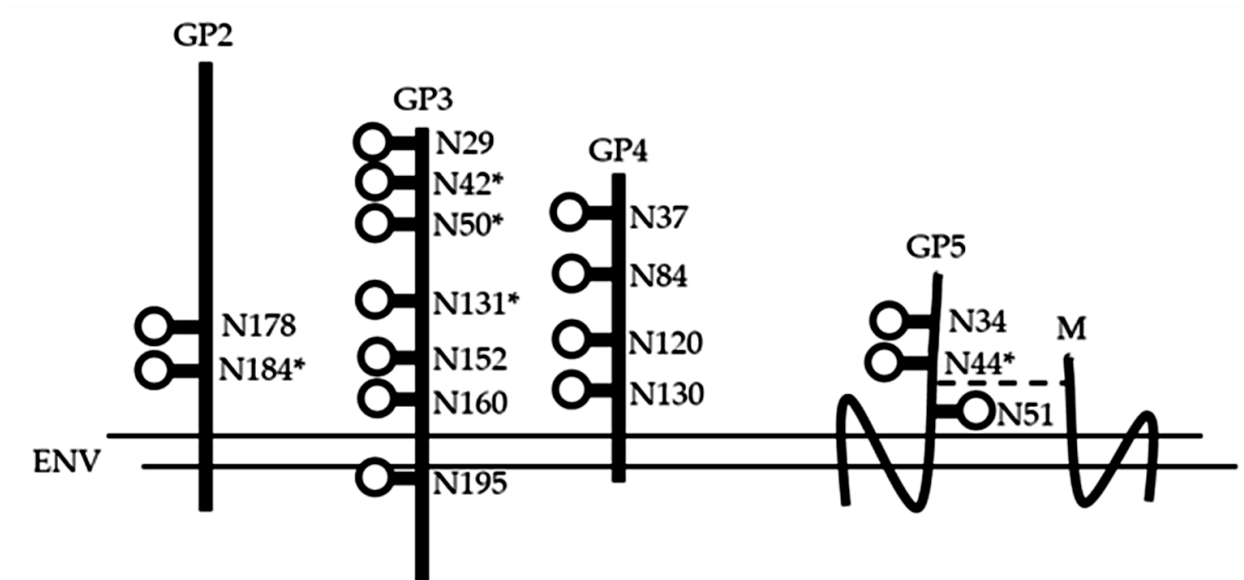


**Figure 1.1. Representation of porcine reproductive and respiratory syndrome virus-2 (PRRSV-2) virion surface proteins.** The proteins are shown for a representative PRRSV-2 isolate. The minor glycoproteins GP2–4 form a heterotrimer protruding from the virion surface. The surface is dominated by GP5-M heterodimers. The M protein is unglycosylated. The position of the glycosylation sites (circles) for GP2–5 are from Das et al. (2011) and Ansari et al. (2006). Asterisks show those N-sites required for infection (Das et al., 2011; Ansari et al., 2006). The dashed line identifies the disulfide bond between GP5 and M. The structures are not drawn to scale.

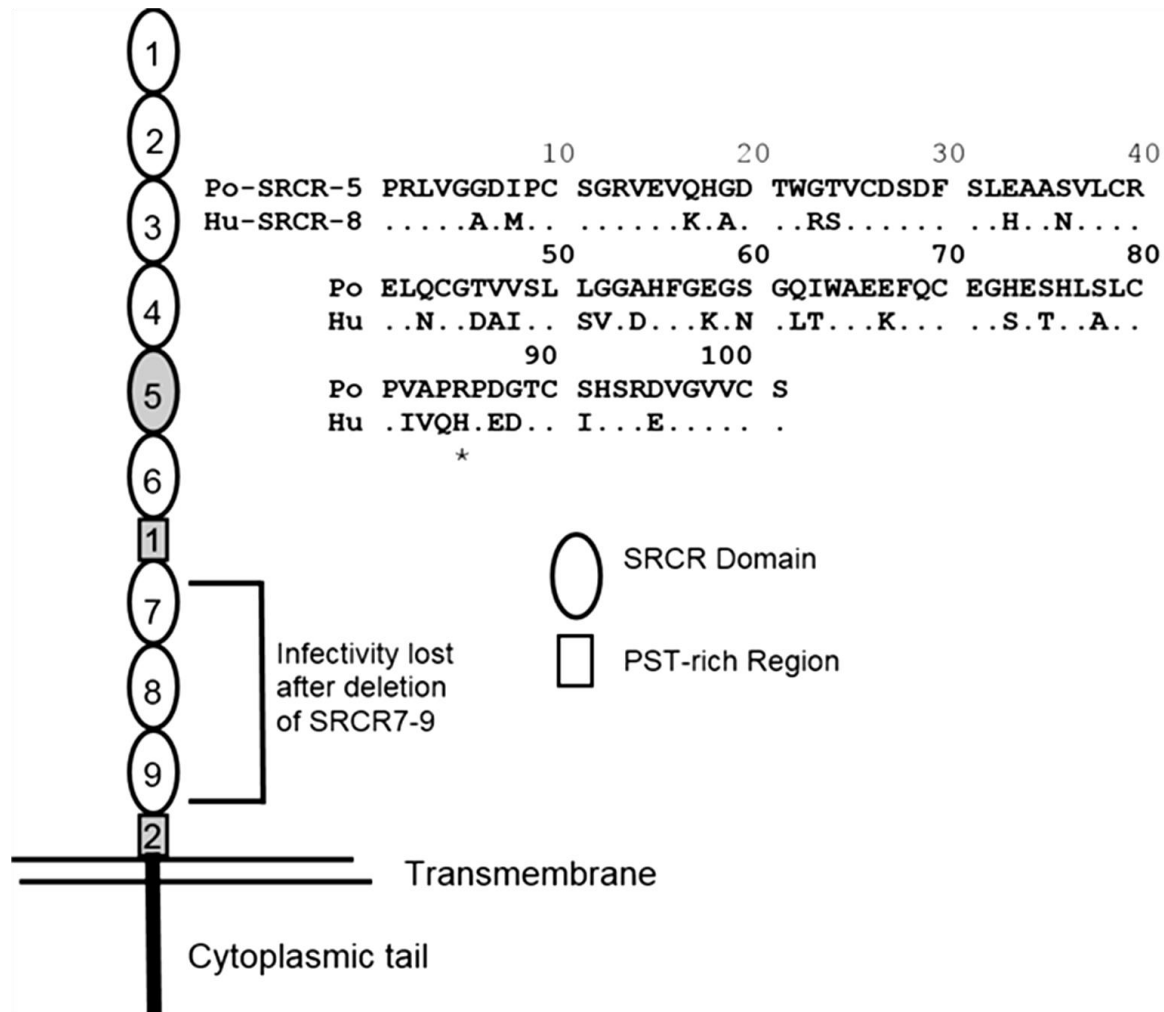


**Figure 1.2. Porcine CD163 organization and SRCR5 peptide sequence.** This illustration shows the location of the different domains in porcine CD163 (pCD163). The shaded regions are domains that participate in PRRSV infection of cDNA transfected human embryonic kidney (HEK) cells (Van Gorp et al., 2010). The peptide sequences show a comparison between SRCR5 of pCD163 and SRCR8 from the human CD163-like protein (Wells et al., 2017). The asterisk shows the location of the R561A mutation described in Ma et al. (2017).

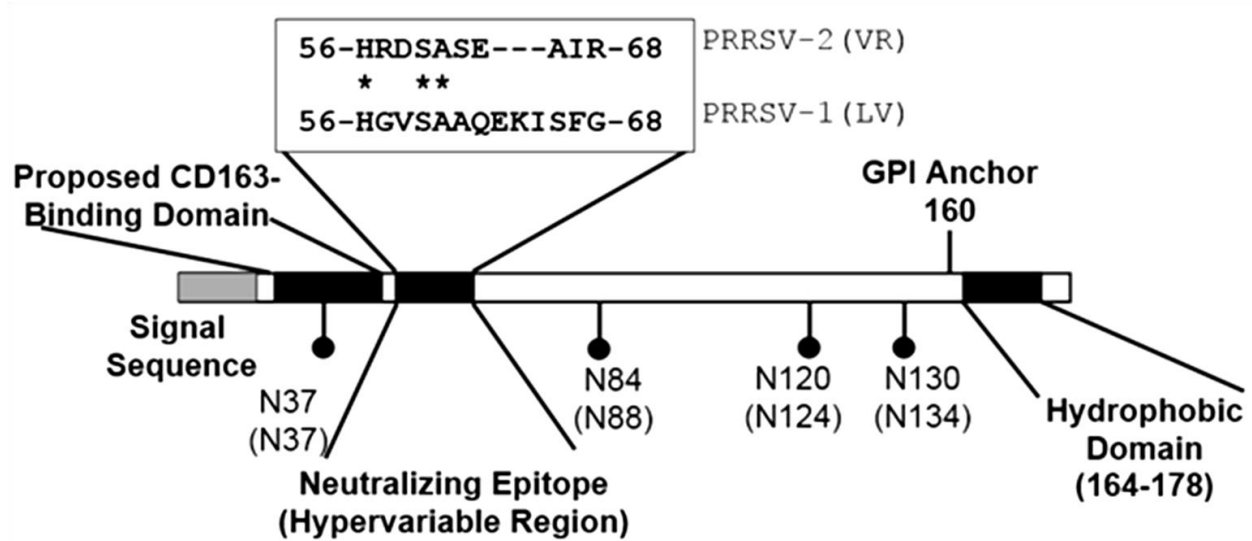


**Figure 1.3. Functional domains in PRRSV GP4.** The locations of the N-glycosylation sites are shown for PRRSV-2 (PRRSV-1 in parentheses). The neutralizing epitope—GP4(56–68)—is described in Vanhee et al. (2010). Asterisks show amino acids shared by PRRSV-1 and PRRSV-2. The GPI anchor for PRRSV-2 and the proposed CD163 binding domains are described in Du et al. (2012) and Chen et al. (2018), respectively. The illustration is based on GP4 from representative PRRSV-1 Lelystad (LV) and PRRSV-2 VR-2332 (VR), GenBank M96262.2 and U87392.3, respectively.

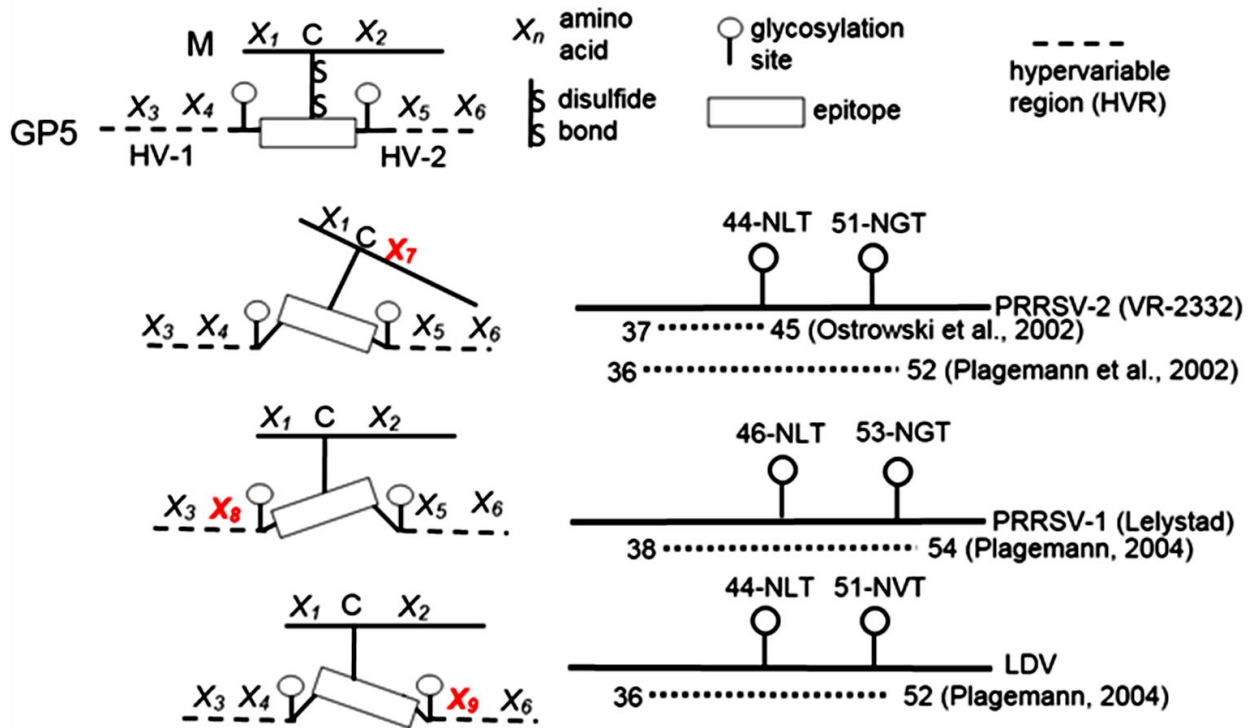


**Figure 1.4. Effect of mutations in GP5 and M proteins on the orientation of a conserved linear epitope.** Amino acid mutations (shown in red) influence the orientation of a conserved linear neutralizing epitope. The mutations are sufficient to block neutralizing antibody without affecting how the oligopeptide functions in its interaction with the host cell. N-glycosylation sites provide further shielding. The right-hand figure shows the location of the N-glycosylation sites (circles) and putative neutralizing epitope (dashed lines) for representative PRRS viruses and for lactate dehydrogenase-elevating virus (LDV).

# **Chapter 2 - Receptor editing approaches for domains and regions of CD163 that are involved in infection with a porcine reproductive and respiratory syndrome virus-2 (PRRSV-2)**

## **INTRODUCTION**

Genetically modified pigs that lack the full-length CD163 receptor on macrophages are completely resistant to PRRSV infection (Whitworth et al., 2016). Since CD163 is involved in heme sequestration which leads to down-regulation of inflammation, deletion of the entire protein would have important negative consequences. A study done by Van Gorp et al. (2010) used an *in vitro* system to identify SRCR5 of CD163 as important for infection with PRRSV-1. In this system, non-permissive HEK293T (HEK) cells were transfected with CD163 constructs possessing different domain deletions and domain swaps from the human CD163-like (hCD163L1) protein. Besides demonstrating the requirement of SRCR5, other domains were identified as important for PRRSV-1 infection, including PSTII, and SRCR6-9.

The purpose of this study was to identify regions in CD163 important for infection with a PRRSV-2 isolate. The approach is similar to the method described in Van Gorp et al. (2010) except that the CD163 cDNA is fused with enhanced green fluorescent protein (EGFP) and the transfected cells are infected with a PRRSV that expresses red fluorescent protein (RFP). Therefore, infection is easily identified by cells with green and red fluorescence. The results showed that transfected cells possessing a deletion of the 101 amino acid SRCR5 or disruption of any of the conserved disulfide bonds within SRCR5 of CD163 were resistant to infection. Deletion of the 16 amino acid PSTII domain also made transfected cells resistant to infection.

The results can be used in the construction of genetically modified pigs that are resistant to PRRSV without affecting CD163's other biological functions.

## **MATERIALS AND METHODS**

**Virus and cells.** The PRRSV-2 isolate was originally derived from an infectious clone of P129 strain that translated a green fluorescent protein (GFP) from a separate subgenomic mRNA (Pei et al., 2009). The GFP was replaced with a red fluorescent protein cDNA (RFP; Chand, 2013). The virus was derived by first transfecting HEK293T (HEK) cells with the P129-RFP infectious clone plasmid DNA and incubated for 48 hrs at 37 °C and 5% CO<sub>2</sub>. The cell culture supernatant from the infectious clone-transfected HEK cells was used for propagation of the virus on MARC-145 cells. Three days after infection of confluent MARC-145 cells, the presence of infection was confirmed by the presence of red fluorescence. The virus was further amplified by passage on MARC-145 cells. For titration of the virus stocks, different passages of viruses were serially diluted 1:10 on 96-well plates of MARC-145 cells. Dilutions were performed in triplicate and the titration endpoint was determined after an incubation for 3 days at 37 °C and 5% CO<sub>2</sub> as the last well showing red fluorescence. The log<sub>10</sub> 50% tissue culture infectious dose (TCID<sub>50</sub>)/ml was calculated according to the method of Reed and Muench (1938). The MARC-145 cells used for virus propagation together with the HEK cells used for transfections were maintained in MEM medium containing 7% FBS, Pen-Strep antibiotics (80 U/ml and 80 µg/ml, respectively) and 3 µg/ml Fungizone.

**Construction of CD163 N-terminal and C-terminal deletion mutants.** The backbone for the preparation of the deletion constructs was a porcine CD163 cDNA (GenBank Acc No. EU016226)

cloned into a pcDNA3.1-EGFP expression vector, which was generously provided by Dr. Dongwan Yoo, University of Illinois. The CD163 cDNA constructs possessing truncations from the N-terminal end were prepared using the primers listed in Table 2.1 and illustrated in Figure 2.1A (see constructs B through H). The primers possessed KpnI and XbaI restriction sites on the 5' and 3' ends, respectively. PCR amplification of the CD163 cDNA was performed using the GoTaqGreen<sup>®</sup> Master Mix (Promega) according to manufacturer's instructions. PCR conditions included 95 °C for 2 min, followed by 30 cycles of 94 °C for 30 s, 65 °C for 30 s, and 72 °C for 2 min, and a final extension at 72 °C for 10 min. The PCR products were cloned into pCR<sup>®</sup>2.1-TOPO<sup>®</sup> vector (Invitrogen) and transformed into One Shot<sup>®</sup> TOP10 chemically competent *E. coli* cells (Invitrogen). The CD163 fragments containing KpnI and XbaI sites were cloned into the KpnI-XbaI sites of the pcDNA3.1-EGFP vector at a 1:3 ratio of vector:insert. Plasmids were transformed into One Shot<sup>®</sup> TOP10 chemically competent *E. coli* cells. Three clones per sample were selected from the overnight plates and transferred into Luria-Bertani (LB) agar with 100 µg/ml of Ampicillin. Clones were screened by double digestion with KpnI and XbaI for the presence of the target insert.

Constructs that possessed deletions at the C-terminal end of the ectodomain region of CD163 (see Figure 2.1A) incorporated primers with PacI restriction sites followed by an additional nucleotide that ensured the in-frame deletion (see Table 2.1). Deletions were made using a long PCR protocol designed to amplify the desired CD163 fragment along with the entire pcDNA3.1-EGFP plasmid (as described above). The PCR products were cut with PacI and the plasmid containing the deleted region re-circularized by ligation with Anza<sup>™</sup> T4 DNA Ligase Master Mix (Invitrogen), and then transformed into One Shot<sup>®</sup> TOP10 chemically competent cells. The resulting CD163 deletion constructs retained intact transmembrane and cytoplasmic

domains along with an additional PacI site (see constructs I through O in Figure 2.1A). Finally, Construct P, which only contained the extracellular SRCR5 and PSTII domains was prepared by incorporating construct D in Figure 2.1 as a backbone for PCR amplification.

**Removal of disulfide bonds in SRCR5.** As illustrated in Figure 2.4, there are eight cysteines that form four disulfide bonds in SRCR5 (Ma et al., 2016). Individual disulfide bonds were removed by substituting one of the partner cysteines with an alanine. Alanine to cysteines substitutions were made for C1, C3, C5 and C7. For C1, C3 and C5, the codons for two existing proline-arginine dipeptides, located at positions 1 and 84 of SRCR5, were changed to SacII sites. The CD163-EGFP plasmid was cut with SacII and the intervening DNA sequence replaced with a synthesized fragment (IDT, Inc.) possessing SacII restriction sites on the ends. The proper orientation of the cDNA insert was confirmed by DNA sequencing. Since C7 is located near the PR-84, the alanine substitution was made by amplifying the plasmid using a unique primer pair possessing SacII restriction sites and the codon for the alanine substitution (see Table 2.1).

**Construction of the Exon 13 and Exon 14 mutants.** The 16 amino acid PSTII is divided into two regions; the Exon 13 region composed of 12 amino acids and the Exon 14 portion consisting of the four amino acids, GRSS, which are on the external surface of the plasma membrane. The remainder of Exon 14 includes the transmembrane domain and a portion of the cytoplasmic tail. The Exon 13 and Exon 14 constructs incorporated primers that possessed SacII restriction sites. The SacII sites were placed in a reading frame to code for alanines. These primers were used to amplify the SRCR domains of interest using the full-length CD163 cloned in the pcDNA3.1-

EGFP expression vector as described above for the CD163 deletion constructs. All constructs retained the N-terminal signal peptide. The primers used for amplification are listed in Table 2.1.

**Transfection of non-permissive HEK cells and infection with a PRRSV-2 isolate.** The CD163-EGFP generated constructs were transfected into HEK cells using FuGENE<sup>®</sup> HD reagent (Promega) according to manufacturer's instructions. Briefly, the day before transfection, cells were plated on 24-well plates at a density of  $8 \times 10^4$  cells/well. When the cells were 80-90% confluent, the mixtures of plasmid and transfection reagent were added into the cell culture. At 24-48 hrs post-transfection, the cells were examined for the presence of EGFP expression under a fluorescence microscope (Nikon ECLIPSE TE2000-S). The transfected HEK cells were infected with the P129-RFP virus at a MOI of approximately 0.1. After 48 hrs, the infection of CD163-expressing cells by PRRSV was clearly evident by the co-localization of green and red fluorescence in the same cell.

**Western blot.** Cell monolayers on 24-well plates transfected with different CD163 plasmids were analyzed by western blot. Two days post-transfection, the cells were washed once with cold PBS and re-suspended in 300  $\mu$ l NP-40 lysis buffer (Invitrogen). The remaining cell material was removed with a cell scraper and transferred to a microcentrifuge tube. After 30 min on ice under constant agitation, the supernatant was removed by centrifugation and proteins separated on a 10% SDS-PAGE gel. The SDS-PAGE gel was rinsed in PBS-Tween 20 (PBST) and the PVDF membrane (0.45  $\mu$ m) was submerged in methanol for membrane activation, followed by rinsing in double-distilled water for 10 minutes. Prior to assembly, the gel, filter paper (0.83 mm) and PVDF membrane were soaked for 20 minutes in 1x transfer buffer (0.03 M glycine, 0.04 M tris

base, 0.04% SDS, and 20% methanol). The blot apparatus was assembled, and electrophoretic transfer performed on a Mini Trans-Blot<sup>®</sup> Electrophoretic Transfer Cell (BIO-RAD) following the manufacturer's instructions. After transfer, the membrane was blocked in PBS with 5% non-fat dry milk (PBS-NFDM) for 1 hr at room temperature (RT). The CD163-EGFP fusion proteins were detected with horseradish peroxidase (HRP)-conjugated goat anti-GFP antibody (R&D Systems), diluted 1:1000 in PBS-NFDM and incubated for 1 hr at RT. Peroxidase activity was visualized using a CN/DAB Substrate Kit (Thermo Scientific Pierce) according to the kit instructions.

**Flow cytometry for surface expression of CD163.** At 48 hrs after transfection with CD163 plasmids, HEK cells were washed twice with PBS and detached with TrypLE<sup>™</sup> Express (ThermoFisher Scientific) according to manufacturer's instructions. Cells were adjusted to a concentration of approximately  $2 \times 10^7$  cells/ml in PBS with 10% mouse serum (PBS-MS) or goat serum (PBS-GS) and a total volume of 100  $\mu$ l of the cell suspension was placed in 12 mm x 75 mm polystyrene flow cytometry tubes. After a 15 min incubation at 4 °C, the cells were pelleted by centrifugation and re-suspended in 100  $\mu$ l of either R-Phycoerythrin (RPE) conjugated mouse anti-porcine CD163 mAb at a concentration of 10  $\mu$ g/ml in 2% PBS-MS (Clone 2A10/11, BIO-RAD) or rabbit anti-CD163 pAb (Biorbyt) followed by incubation with goat anti-rabbit Alexa Fluor 647 (AF647) conjugate. After a 30 min incubation on ice, the cells were washed twice with 2% PBS-MS/GS, brought to a final volume of 300-500  $\mu$ l and analyzed on the BD LSR Fortessa X-20 Flow Cytometer (BD Biosciences) with FCS Express 5 software (De Novo Software). A minimum of 10,000 cells were analyzed for each sample. Unstained, GFP-only and RPE/AF647-

only samples along with an isotype control consisting of HEK cells stained with an RPE-conjugated mouse IgG1 negative control (BIO-RAD) were included in each experiment.

## RESULTS

### **Infection of HEK cells transfected with CD163 deletion mutants.**

The experimental system used in this study incorporated a CD163-EGFP fusion protein expressed in HEK cells followed by infection with a PRRSV-2 isolate expressing RFP. As shown in Figure 2.2, infection of CD163 receptor-expressing cells is easily identified by the colocalization of green and red fluorescence. The CD163 deletion constructs tested for PRRSV-RFP permissiveness are shown in Figure 2.1A. All constructs produced EGFP fluorescence within 48 hrs after transfection. Western blots stained with anti-GFP antibody confirmed that all CD163-EGFP proteins migrated according to their predicted size (Figure 2.1C).

As shown in Figure 2.1B, the N-terminal deletion mutants B, C and D, which retained the SRCR5 domain were positive for infection; whereas, the constructs E, F, G, which lacked SRCR5, were negative for infection. The results for the C-terminal deletions lacking the PSTII domain (constructs I, J, K), were negative for infection; even though constructs J and K retained the SRCR5 domain. Constructs N and O, which were identical to J and K, but retained the PSTII domain were positive for infection. Construct O, which lacked domains 8 and 9, showed reduced infection compared to the wild-type CD163, Construct A. Construct P, which possessed only SRCR5 and PSTII as external domains, was positive for infection, but at a greatly reduced level. Staining live cells with anti-CD163 antibodies followed by flow cytometry confirmed that all constructs expressed CD163 on the HEK cell surface (see Figure 2.3). The only exceptions were

Construct H, which lacked the transmembrane domain for anchoring CD163 to the cell surface; and Construct P, which lacked the epitopes recognized by the CD163 antibodies.

When taken together, the results showed that SRCR5 and PSTII are the major domains required for infection with a PRRSV-2 isolate. Using a PRRSV-1 isolate, Van Gorp et al. (2010) reported the same requirements for SRCR5 and PSTII.

### **All disulfide bonds in SRCR5 are required for infection.**

As illustrated in Figure 2.4A, SRCR5 is predicted to possess four disulfide bonds formed by the eight cysteine residues located at amino acid positions 10, 26, 39, 44, 70, 80, 90 and 100. To investigate the role of disulfide bonds for PRRSV-2 infection, we removed individual disulfide bonds by replacing the cysteines at C1, C3, C5 or C7 with alanine. As summarized in Figure 2.4A, HEK cells transfected with the wild-type CD163 showed an infection rate of 61.2% of EGFP expressing cells compared to 0.8% for the alanine substitution at C1; 1.0% for the alanine substitution at C3; 1.2% for the alanine substitution at C5; and 1.3% for the alanine substitution at C7. In order to confirm that the negative result in infection was due to the lack of interaction with the PRRSV proteins and not due to the lack of surface expression, the constructs bearing cysteines to alanine mutations were assessed by flow cytometry. As shown in Figure 2.4B, all constructs showed similar levels of surface expression when compared to the WT after staining with the anti-CD163 mAb 2A10. These data showed that the disruption of any of the disulfide bonds results in a dramatic reduction in infection and provides an explanation for the protective effect of the partial deletion. Guo et al (2019) showed that deletion of a 41 aa region within SRCR5 renders pigs resistant to PRRSV-2 infection. This data supports our hypothesis, as deletion of this region corresponds to the elimination of three out of four disulfide bonds.

### **Contributions of Exon 13 and 14 of PSTII to permissiveness.**

The results in Figure 2.1 predict that PSTII is required for infection with a PRRSV-2 isolate. Therefore, we prepared a CD163 construct that lacked PSTII. As illustrated in Figure 2.5A and 2.5B, the 16 amino acid PSTII domain of porcine CD163 is composed of 12 amino acids contributed entirely by Exon 13 combined with four amino acids, GRSS, contributed by Exon 14. With this structure in mind, the removal of Exon 13 provides a convenient means to genetically modify CD163. The contribution of the four amino acid peptide sequence in Exon 14 to infection was evaluated by replacing GRSS with three alanines (see Construct R in Figure 2.5B). The rationale for inserting the alanines was to create a spacer between SRCR9 and the cell surface. As shown in Figure 2.5B, constructs A and Q were positive for infection, although construct Q showed a lower level of infection compared to the WT CD163. In contrast, construct R was negative for infection (Figure 2.5B). The negative infection result for construct R could be the product of the absence of CD163 expression on the cell surface, a result of removing the PSTII linker domain, located near the transmembrane. Therefore, transfected cells were stained with anti-CD163 mAb, 2A10. All constructs showed surface levels of CD163 expression similar to WT CD163 (see Figure 2.5C).

## **SUMMARY AND CONCLUSIONS**

The genetic modification of pigs lacking CD163 expression on macrophages results in the resistance of macrophages to infection with PRRSV-1 and PRRSV-2 isolates (Whitworth et al., 2016). At the molecular level, the deletion of CD163 PSTII or SRCR5 domains in CD163 is sufficient to block the infection of CD163-transfected HEK cells (see Figure 2.1 and Van Gorp et al. (2010)). The importance of SRCR5 is further evident by the inability of macrophages from

genetically modified pigs to support infection with PRRSV-1 and PRRSV-2 isolates (Burkard et al., 2017). In addition, Yu et al. (2020) generated SRCR5 deletion in MARC-145 cells using CRISPR-Cas9 to show the requirement of SRCR5 in PRRSV-2 infection. However, a distinct difference between PRRSV-1 and PRRSV-2 is found in how the SRCR5 domain is recognized (Wells et al., 2017). For example, alveolar macrophages from pigs possessing a domain swap between porcine CD163 SRCR5 and hCD163LI homolog SRCR8 support infection with PRRSV-2, but not PRRSV-1 isolates.

To better understand the difference in how PRRSV-1 and PRRSV-2 recognize CD163, experiments were performed to determine the effect of domain deletions in CD163 on transfected HEK cells infected with PRRSV-2. This study shows that the requirement of SRCR5 or PSTII domain deletions on PRRSV infection is similar for PRRSV-1 and PRRSV-2 isolates. The deletion of other domains, such as SRCR7, 8 and 9, had a lesser effect on infection. Van Gorp et al., 2010 observed similar results using a PRRSV-1 isolate. Therefore, these data indicate that the difference between PRRSV-1 and PRRSV-2 in the recognition of CD163 locates to SRCR5.

In addition to making whole deletions in SRCR5, Guo et al (2019) showed that making a partial 41 bp deletion in SRCR5 was sufficient to provide resistance of pigs to PRRSV-2 infection. The rationale for preparing the partial deletion was to eliminate a ligand binding pocket domain. However, an alternative explanation for resistance conferred by the 41 amino acid deletion is the removal of conserved disulfide linkages, which are required to maintain the tertiary structure of the cysteine rich SRCR5 domain. The crystal structure of SRCR5 polypeptide shows four disulfide bonds, which are formed by C1-C4, C2-C7, C3-C8, and C5-C6

linkages. As illustrated in Figure 2.4, the 41 amino acid deletion eliminates three of the four disulfide bonds.

The current model for the interaction between CD163 and PRRSV involves the participation of a minor population of heterotrimers formed by the surface glycoproteins, GP2, GP3 and GP4 (Das et al., 2010). GP2 and GP4 are co-precipitated with CD163 in pull-down assays. The surface of the virion is also heavily populated by GP5-M homodimers. The fact that both PSTII and SRCR5 are required for infection, but spatially separated from each other within the CD163 protein, suggests that multiple viral envelope proteins may form multiple contacts with CD163.

**Table 2.1. Primers for amplification of CD163 constructs shown in Figure 2.1. The underlined nucleotides identify restriction sites; in italics is represented the nucleotide that was added after the *PacI* site to ensure an in-frame construct.**

<b>Construct</b>	<b>Primer Sequence</b>
B	F- <u>GGT</u> ACCATGGGATCTGATTTAGAGATGAGG R- <u>TCTAGATT</u> GTA <del>CTTCAGAGTGGTCTCC</del>
C	F- <u>GGT</u> ACCATGGGAGCAGACCTGAAACTG R- <u>TCTAGATT</u> GTA <del>CTTCAGAGTGGTCTCC</del>
D	F- <u>GGT</u> ACCATGCACAGGAAACCCAGGC R- <u>TCTAGATT</u> GTA <del>CTTCAGAGTGGTCTCC</del>
E	F- <u>GGT</u> ACCATGTACACACAAATCCGC R- <u>TCTAGATT</u> GTA <del>CTTCAGAGTGGTCTCC</del>
F	F- <u>GGT</u> ACCATGAGTGGTCAACTTCGCTG R- <u>TCTAGATT</u> GTA <del>CTTCAGAGTGGTCTCC</del>
G	F- <u>GGT</u> ACCATGAAAATAAGACTTCAAGAAGGAAACACT R- <u>TCTAGATT</u> GTA <del>CTTCAGAGTGGTCTCC</del>
H	F- <u>GGT</u> ACCATGGGAAAAGACAAGGAG R- <u>TCTAGATT</u> CTGAGCACGTCACAGC
I	F-ATTATTAATTAAGTTTGTGCACTTGCAATCTTTGGGGT R-ATCATTAATTA <del>AATTTAAGCAAATCACTCCAGCATCCTCAG</del>
J	F-ATTATTAATTAAGTTTGTGCACTTGCAATCTTTGGGGT R-ATCGTTAATTA <del>A</del> CTTTGAGCAGACTACGCCG
K	F-ATTATTAATTAAGTTTGTGCACTTGCAATCTTTGGGGT R-CAGTTAATTA <del>A</del> CTCTGAGCAGATGACTCCTGC
L	F-CACTTTAATTAAGTACACACAAATCCGCTTGGTGAATG R-CATATTAATTA <del>A</del> GGCTGAGCAGGTAATTTTGGCTTC
M	F-ATTATTAATTAAGATTGCAAAGAGCCGAGAATCCCTACATG R-ATCATTAATTA <del>A</del> AATTTAAGCAAATCACTCCAGCATCCTCAG
N	F-ATTATTAATTAAGATTGCAAAGAGCCGAGAATCCCTACATG R-ATCGTTAATTA <del>A</del> TCTTTGAGCAGACTACGCCG
O	F-ATTATTAATTAAGATTGCAAAGAGCCGAGAATCCCTACATG R-CAGTTAATTA <del>A</del> CTCTGAGCAGATGACTCCTGCCGAGGAGTCATCTGCTGA
P	F-ACACCCGCGGAAATTGCAAAGAGCCGAGAATCCCTACA R-CCACCCGCGGTGAGCAGACTACGCCGACGTCCC
Q	F-CACACCCGCGGCTTTTGTGCACTTGCAATCTTTGGGGTCATTCTGT R-CCCACCCGCGGCTGTGGCATGTAGGGATTCTCGGCTCTTT
R	F-CACACCCGCGGTCGCTCATCTTTTGTGCACTTGCAATCTTT R-AACACCCGCGGCTGAGCACGTCACAGCAGCATCCT
C7 to A	F-CAACCCGCGGCCTGACGGGACAGCCAGCCAC R-ACAACCCGCGGTGCTACTGGGCAGAGTGAAAGGTGGGACTC

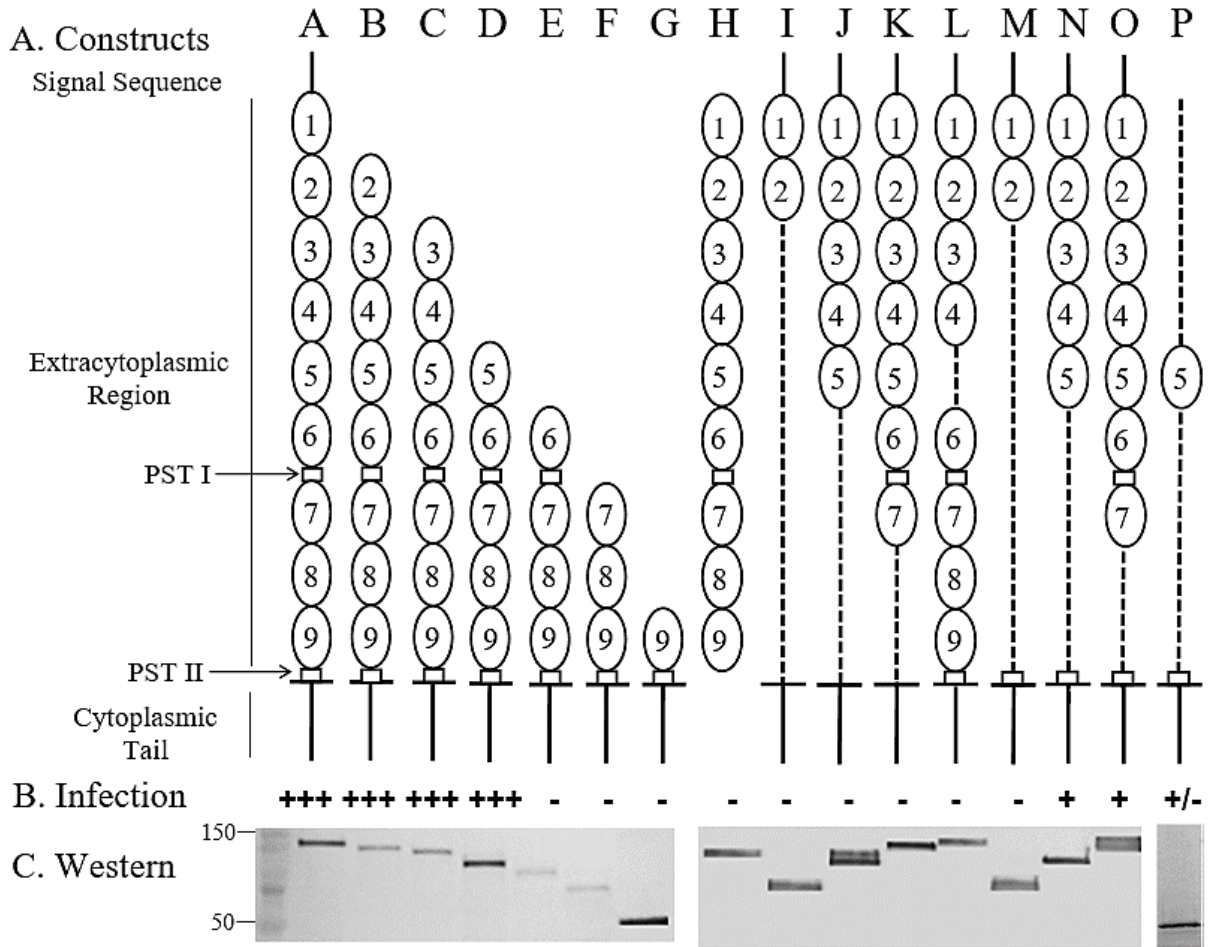


**Figure 2.1. CD163 constructs used to identify domains involved in PRRSV-2 infection.** (A) Deletion mutants used in the transfection of HEK cells. Ovals and squares identify the SRCR and PST domains, respectively. (B) Result for PRRSV infection of transfected HEK cells. Key: (+++), similar to results for wild-type CD163 including numerous large clusters of infected cells; (++) , several small clusters of infected cells; (+), multiple single infected cells, but no clusters; (+/-), a few scattered infected cells; (-), no detectable infected cells. (C) Results for western blots using anti-GFP antibody for the detection of the CD163-EGFP fusion proteins.

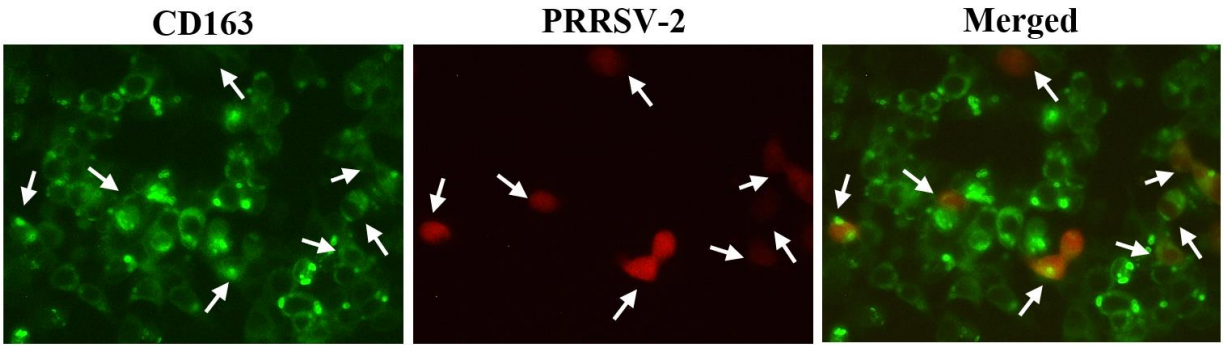


**Figure 2.2. Co-localization of CD163-EGFP and P129-RFP in HEK cells.** Non-permissive HEK cells were transfected with different CD163 deletion constructs (represented in green). At 24-48 hrs post-transfection, the cells were infected with P129-RFP (represented in red). A positive result for infection is recorded as a cell expressing both green and red fluorescence.

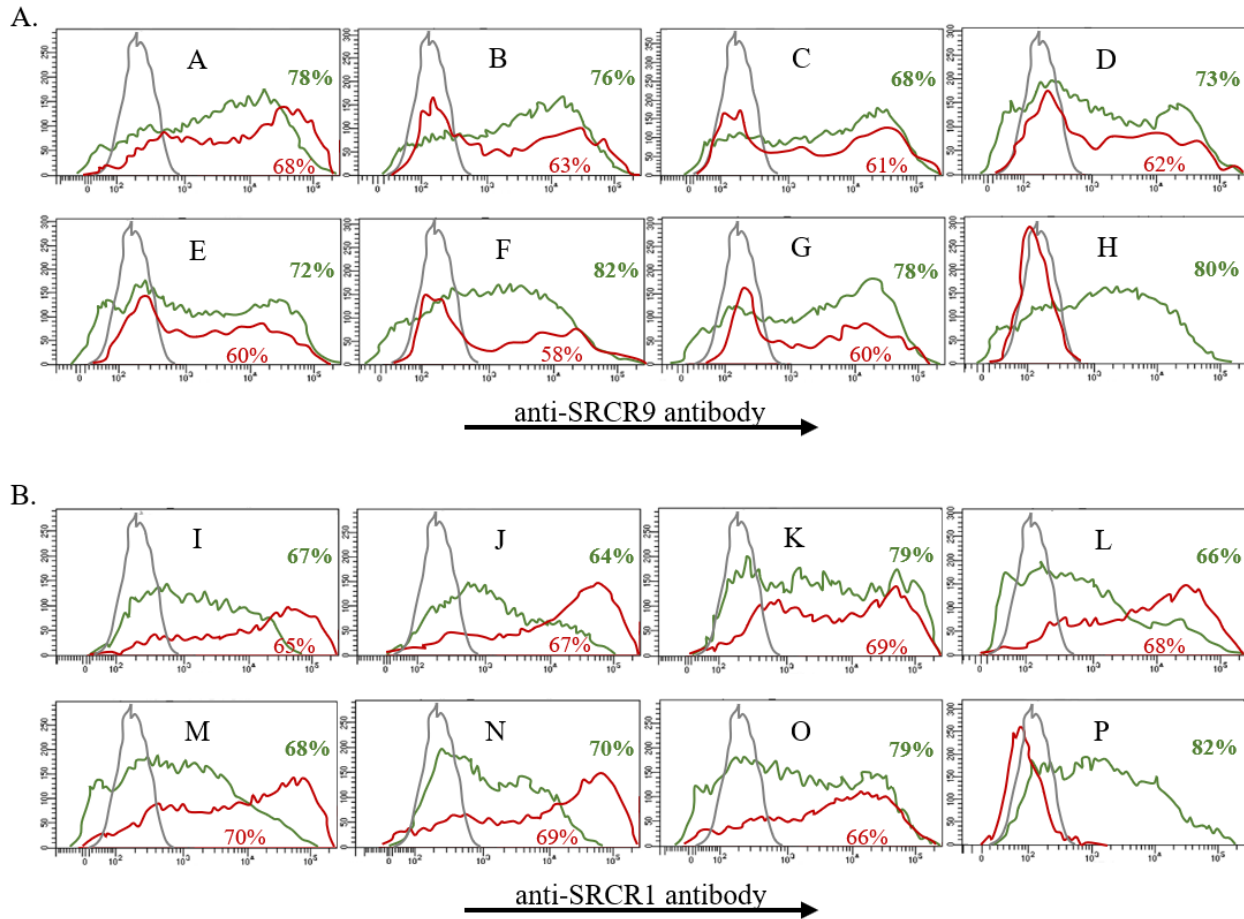


**Figure 2.3. Surface expression of CD163 constructs expressed in transfected HEK cells.** Letters refer to the constructs shown in Figure 2.1A. The top row of histograms are cells stained with a rabbit anti-CD163 antibody prepared against an oligopeptide in SRCR9 (Biorbyt). The bottom histograms show cells stained with a mouse mAb 2A10 (BIO-RAD). The GFP expression is represented in green, the mAb 2A10 staining in red and the isotype control in gray. Cells were stained 48 hrs after transfection. The CD163 staining results are shown as percentage of CD163-positive cells from the GFP-positive gated population.

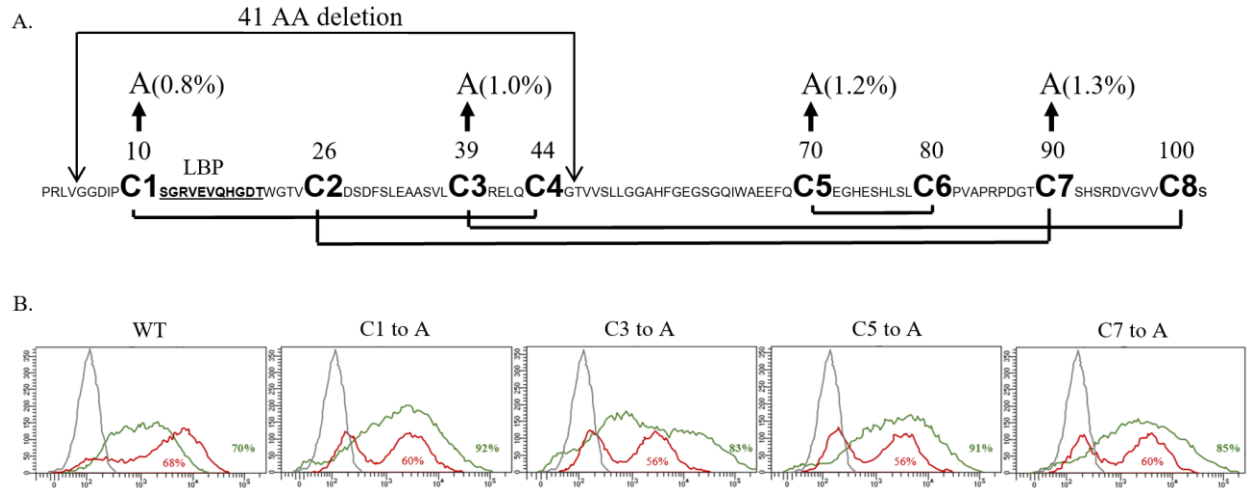


**Figure 2.4. Effect of cysteine to alanine substitutions in SRCR5 on PRRSV infection.** (A) Disulfide bonds in SRCR5 were removed by making cysteine to alanine substitutions at C1, C3, C5 or C7. The locations of the different disulfide bonds are according to Ma et al. (2016). The number above each cysteine is the location within the SRCR5 peptide sequence. The number in parentheses is the fraction of infected cells compared to the wild-type CD163 as the positive control. All infections were performed on the same 24-well plate. The percent of green cells infected for the wild-type CD163 was 61.2%. The locations of the 41 amino acid deletion described by Guo et al. (2019) and ligand binding pocket (LBP; bold underlined letters) are identified in the SRCR5 peptide sequence. (B) shows the surface expression of CD163 for the cysteine to alanine mutated constructs. The GFP expression is represented in green, the mAb 2A10 staining in red and the isotype control in gray. Cells were stained 48 hrs after transfection. The mAb 2A10 staining results are shown as percentage of CD163-positive cells from the GFP-positive gated population.

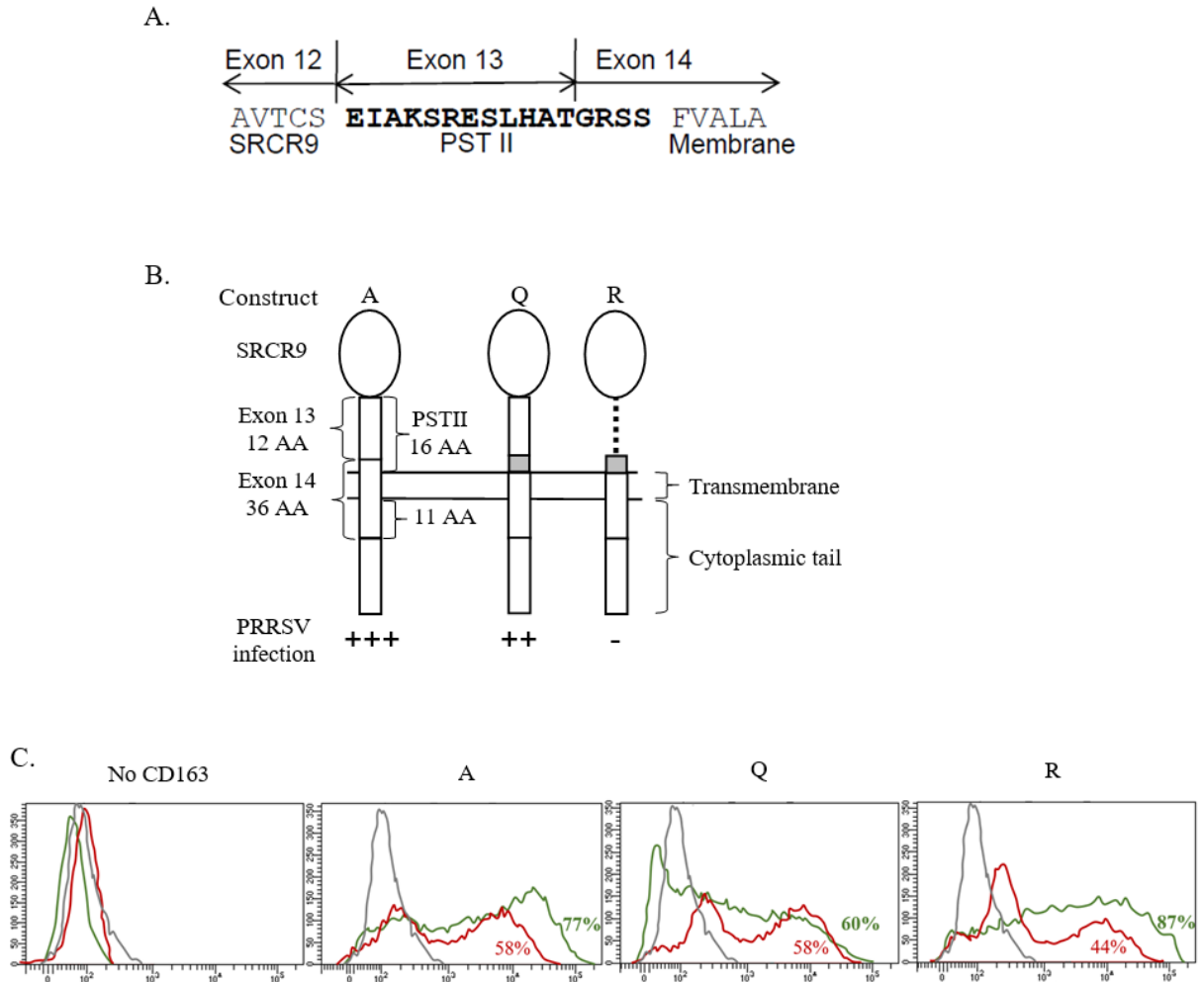


**Figure 2.5. Infection of HEK cells expressing CD163 PSTII constructs.** (A) shows the peptide sequence for the PSTII region covered by Exons 12, 13 and 14. The letters in bold show the amino acid of the PSTII domain. (B) is a diagram of the PSTII constructs used for transfection of HEK cells. The shaded box shows the location of the substitution of the GRSS peptide sequence with three alanine residues. The key for infection is the same as described in Figure 2.1. (C) shows the surface expression of CD163 for the PSTII constructs. The GFP expression is represented in green, the mAb 2A10 staining in red and the isotype control in gray. Cells were stained 48 hrs after transfection. The mAb 2A10 staining results are shown as percentage of CD163-positive cells from the GFP-positive gated population.

# **Chapter 3 - Peptide sequences in scavenger receptor cysteine rich (SRCR) protein domain 5 of porcine CD163 involved in infection with a porcine reproductive and respiratory syndrome virus (PRRSV)**

## **INTRODUCTION**

Work by us and others (Van Gorp et al., 2010) showed the importance of SRCR5 for infection with both PRRSV-1 and PRRSV-2 viruses. These results are supported by two recent reports. Burkard et al. (2017) showed that pulmonary alveolar macrophages (PAMs) or peripheral blood monocyte-derived macrophages (PDMs) from genetically modified pigs possessing a complete deletion of SRCR5 are resistant to infection with both viruses. Ma et al. (2016) carried out structure-based mutational studies to identify that the arginine residue at position 561 (Arg561) in the long loop region of SRCR5 is important for infection with two PRRSV-2 isolates.

Wells et al. (2017) demonstrated that the substitution of CD163 SRCR5 with the human CD163 like (hCD163L1) protein rendered macrophages and pigs resistant to infection with PRRSV-1 isolates. However, pigs with the hCD163L1 domain swap retained the ability to support replication of PRRSV-2 viruses. These results show that PRRSV-1 and PRRSV-2 recognize different peptide sequences within SRCR5 of CD163. Therefore, the overall goal was to identify the minimum changes in SRCR5 sufficient to make cells resistant to infection with PRRSV. Proline-arginine insertions (PR) in the SRCR5 polypeptide were used to identify

regions involved in infection of transfected HEK293T (HEK) cells with PRRSV-1 or PRRSV-2 isolates.

An analysis of previous studies that demonstrated the requirement of SRCR5 for infection showed that some SRCR5 deletion constructs retained the ability to sustain a low-level of infection when retaining the SRCR4/5 inter-domain region, alanine-histidine-arginine-lysine (AHRK). Therefore, mutations were created in the inter-domain region of a CD163-EGFP construct. After transfection onto HEK cells, the permissiveness of each mutation was assessed by infection with two PRRSV isolates.

The results from this study showed that the insertion of proline-arginine (PR) after amino acids 57 and 99 inhibits infection with a PRRSV-1 isolate, whereas insertion of PR dipeptides after amino acids 8, 54 and 99, inhibits PRRSV-2 infection. Furthermore, the deletion of the SRCR4/5 interdomain sequence, AHRK, also blocks infection. Together, these mutant constructs provide a means to express CD163 receptors that are resistant to PRRSV infection.

## MATERIALS AND METHODS

**Viruses and cells.** The PRRSV-1 isolate, Lelystad, was grown on MARC-145 cells in media containing 7% FBS, Pen-Strep antibiotics (80 U/ml and 80 µg/ml, respectively), 3 µg/ml Fungizone, and 25 mM HEPES for 3 days at 37 °C in 5% CO<sub>2</sub>. The resulting virus were titrated on 96-well plates of MARC-145 cells by preparing 10-fold dilutions in a total volume of 200 µl per well. Dilutions were performed in triplicate and the titration endpoint was determined as the last well showing cytopathic effect (CPE). The log<sub>10</sub> 50% tissue culture infectious dose (TCID<sub>50</sub>)/ml was calculated according to the method of Reed and Muench (1938). The PRRSV-2 isolate, a P129 strain expressing a red fluorescent protein (RFP; Chand, 2013), was propagated

and titered on MARC-145 cells similarly to the PRRSV-1 strain. The titration endpoint was determined as the last well showing red fluorescence. All cell lines used in this study were maintained in MEM medium with 7% FBS and antibiotics.

**Preparation of AHRK SRCR4/5 interdomain constructs.** The CD163 constructs used to study mutations within SRCR4/5 interdomain are described in Table 3.2. The backbone for the preparation of the constructs was a porcine CD163 cDNA (GenBank Acc No. EU016226) cloned into a pcDNA3.1-EGFP expression vector generously provided by Dr. Dongwan Yoo, University of Illinois. The mutations were obtained by using the PCR primers listed in Table 3.1 and a LongAmp<sup>®</sup> *Taq* DNA Polymerase kit (New England Biolabs Inc.). PCR conditions included 94 °C for 30 s, followed by 30 cycles of 94 °C for 30 s, 65 °C for 1 min, and 65 °C for 8 min, followed by a final extension at 65 °C for 10 min. The PCR products were re-circularized by ligation with Anza<sup>™</sup> T4 DNA Ligase Master Mix (Invitrogen) according to manufacturer's instructions. Plasmids were transformed into One Shot<sup>®</sup> TOP10 chemically competent *E. coli* cells (Invitrogen). Three clones per sample were selected from the overnight plates and transferred into Luria-Bertani (LB) agar with 100 µg/ml of Ampicillin. The successful mutation of each construct was confirmed by DNA sequencing.

**Insertional mutagenesis of SRCR5.** The insertion of proline-arginine (PR) dipeptides was accomplished by the in-frame insertion of a *SacII* restriction site into the pcDNA3.1-EGFP expression vector. The primers are listed in Table 3.3. The intact pcDNA3.1 CD163-EGFP plasmid was used as PCR template and the entire plasmid amplified using LongAmp<sup>®</sup> *Taq* DNA Polymerase as described above. The PCR products were cut with *SacII* and the plasmid re-

circularized by ligation with Anza™ T4 DNA Ligase Master Mix (Invitrogen) according to manufacturer's instructions. Plasmids were transformed into One Shot® TOP10 chemically competent *E. coli* cells. Constructs were screened by double digestion with SacII and XbaI, in order to confirm the addition of the SacII restriction site.

**Transfection and infection of HEK cells.** Different CD163-EGFP deletion constructs were transfected into HEK cells using FuGENE® HD reagent (Promega) as described below. The day before transfection, HEK cells were plated on 24-well plates at a density of  $8 \times 10^4$  cells/well and after reaching 80-90% confluency, the mixtures of plasmid and transfection reagent were added into the cell culture. After transfection, the cells were examined daily for the presence of EGFP expression under a fluorescence microscope. Forty-eight hrs post-transfection, the cells were infected with either Lelystad or P129-RFP at a MOI of approximately 0.1. The PRRSV-2 infected cells were detected by the co-localization of green and red fluorescence in the same cell.

At 3 days post-infection with Lelystad virus, the cells were washed with PBS and fixed for 10 min with 4% paraformaldehyde at room temperature (RT), followed by permeabilization with 0.1 Triton-X for 5 min at RT. For detection of infected cells, the wells were stained with PRRSV N-protein-specific mAb (SDOW-17; Rural Technologies Inc.) diluted 1:1000 in PBS with 1% FBS (PBS-FBS) (Sigma-Aldrich). After 1 hr of incubation at 37 °C, the cells were washed with PBS and stained with Alexa Fluor 594-labeled anti-mouse IgG (Thermo Fisher Scientific) diluted 1:400 in PBS-FBS. The plates were incubated for 30 min in the dark at 37 °C, washed with PBS, and viewed under a fluorescence microscope.

**PRRSV-2 titration on transfected HEK cells and preparation of growth curves.** CD163 WT, PR-9, PR-55 and PR-100 constructs were transfected into HEK cells using FuGENE<sup>®</sup> HD reagent as described above. At 48 hrs post-transfection, the cells were infected with 10-fold serial dilutions of the P129-RFP recombinant virus at a starting concentration of  $6.5 \log_{10} \text{TCID}_{50}/\text{ml}$ . After 48 hrs of incubation at 37 °C in 5% CO<sub>2</sub>, the RFP-positive cells were counted in each well and the results were shown as percent infection of CD163-positive cells after 3 individual experiments in comparison to the wild-type.

**Growth curve experiment.** The wild-type, PR-9, PR-55 and PR-100 constructs were transfected on HEK cells as previously described. After 48 hrs, the cells monolayers were infected in quadruplicate with passage 3 of the P129-RFP recombinant virus at a 1:10 dilution for a final volume of 1 ml/well. After 2 hrs of incubation at 37 °C in 5% CO<sub>2</sub>, the inoculum was removed, the cells were washed twice with PBS and fresh media was added to the cells. At 3, 12, 24, 36, and 48 hrs post-infection, 200 µl were removed from each well and placed at -80 °C. The virus stocks were thawed and clarified by centrifugation at 1100 x g for 10 minutes. The virus was then serially diluted at 10-fold dilutions and was used to infect MARC-145 monolayers of cells on 96-well plates in triplicate. After incubation for 3 days at 37 °C in 5% CO<sub>2</sub>, the titration endpoint was determined as the last well showing red fluorescence. The  $\log_{10}$  50% tissue culture infectious dose (TCID<sub>50</sub>)/ml was calculated according to the method of Reed and Muench (1938).

**Measurement of surface expression of CD163 on transfected HEK cells.** Forty-eight hours post-transfection, cells were washed twice with PBS, detached with TrypLE<sup>™</sup> Express

(ThermoFisher Scientific) and approximately  $2 \times 10^7$  cells/mL were re-suspended in PBS with 2% mouse serum (PBS-MS) and placed in 12 mm x 75 mm polystyrene flow cytometry tubes. Cells were pelleted by centrifugation and re-suspended in 100  $\mu$ l of 10% PBS-MS. After a 15 min incubation at 4 °C, the cells were pelleted by centrifugation and re-suspended in 100  $\mu$ l of R-Phycoerythrin (RPE) conjugated mouse anti-porcine CD163 mAb at a concentration of 10  $\mu$ g/ml in 2% PBS-MS (Clone: 2A10/11, BIO-RAD). After a 30 min incubation at 4 °C, the cells were washed twice with 2% PBS-MS and brought to a final volume of 300-500  $\mu$ l and analyzed on the BD LSR Fortessa X-20 Flow Cytometer (BD Biosciences) with FCS Express 5 software (De Novo Software). A minimum of 10,000 cells were analyzed for each sample. Unstained, GFP-only and RPE-only samples along with an isotype control consisting of HEK cells stained with an RPE-conjugated mouse IgG1 negative control (BIO-RAD) were included in each experiment.

**Model prediction of the effect of PR insertions.** Coordinates for CD163 SRCR5 were located through the RCSB Protein Data Bank (PDB code 5JFB; deposited by Ma et al. (2016)). The structural predictions for the proline-arginine (PR) insertion mutations were generated using the PyMOL molecular graphics and modeling system (DeLano, 2002). The I-TASSER V5.1 simulator (Yang et al., 2015) was used for the refinement of the predicted conformational changes. C-scores between 1.0 and 2.0 were considered highly accurate. For simulations that gave multiple model structures, the prediction with the highest C-score value was chosen. For visualization, the generated structures were loaded into the open source program, UCSF Chimera (Pettersen et al., 2004).

## RESULTS

### **The effects of modifications in the SRCR4/5 interdomain peptide sequence, AHRK, on infection.**

The peptide sequence, AHRK, is located between SRCR4 and SRCR5 domains. Table 3.2 shows the effect of mutations in AHRK on PRRSV-1 and PRRSV-2 infection. CD163 construct B, which possesses a complete deletion of AHRK produced a dramatic reduction in infection with both PRRSV-1 and PRRSV-2. However, there were several differences between viruses. For example, PRRSV-2 infection with HEK cells expressing the substitution of AHRK with AAAA (construct C) showed reduced infection. Further substitution of AHRK with AAAK (construct D), AARA (construct E), or AKKK (construct J) produced similar results. Examples of how the insertion of an amino acid can affect infection are found in the results for constructs L and M. However, when probed against a PRRSV-1 isolate, only constructs B and G showed a great impact on infection when compared to the WT (construct A). All constructs showing a reduced level of infection were further tested by flow cytometry for expression of CD163. As shown in Figure 3.1, all inter-domain constructs showed high levels of CD163 surface expression. Together, these results demonstrate that amino acid deletions, insertions and substitutions within the SRCR4/5 interdomain region affect the ability of CD163 to function as a receptor for PRRSV.

### **The effects of PR dipeptide insertions in SRCR5 on PRRSV-2 infection.**

The approach for probing the regions within SRCR5 involved in infection incorporated the insertion of single PR dipeptides located about every 10 amino acids along the 101 amino polypeptide sequence. The results after infection of transfected HEK cells with P129-RFP,

summarized in Figure 3.2, showed a wide range of infection rates. In general, PR insertions located in the N-terminal half of the SRCR5 polypeptide had a greater impact on infection than the mutations in the C-terminal half. Three PR insertions, PR-9, PR-55 and PR-100, produced the greatest reduction in infection, with only a small percentage of CD163-EGFP cells showing RFP fluorescence after 48 hrs. One possibility for decreased infection was that CD163 may not have been expressed on the surface of the transfected HEK cells; thereby, preventing access of the virus to the receptor. However, staining with the anti-CD163 mAb 2A10 by flow cytometry confirmed that the mutant CD163 proteins were expressed on the cell surface (see Figure 3.3).

A more detailed analysis of the effect of the PR-9, PR-55 and PR-100 mutations on PRRSV-2 infection was performed by conducting titration endpoint and growth curve experiments on HEK cells expressing the different mutated CD163 proteins. Results for three independent experiments, presented in Table 3.4, showed that for the WT CD163, 59.3% +/- 3.6 of EGFP-expressing cells were infected in the first well with an endpoint of  $10^{-4}$  for two out of the three experiments. In contrast, the infection of HEK cells expressing PR-9, PR-55 or PR-100 constructs showed only a few infected cells at the initial concentration of virus (between 0.8% and 3.0% of infected EGFP-positive cells) and the endpoints for PR-9 and PR-100 were  $10^{-2}$ . The titration endpoint for PR-55 was  $10^{-1}$ . The results for the titration experiments were supported by growth curves, shown in Figure 3.4. After infection for one hr and washing, the residual virus remaining in the well was 4  $\log_{10}$  TCID<sub>50</sub>/ml for the mutant CD163 constructs. The concentration of virus for HEK cells transfected with the wild-type CD163 increased over time; reaching a peak of 7  $\log_{10}$  TCID<sub>50</sub>/ml, which represented a 3-log increase in virus concentration. In contrast, virus infection of the PR mutants showed no increase in virus over time. In fact, the amount of virus decayed, reaching undetectable levels for all three CD163 mutants by 36 hrs

after infection. These data show that cells expressing PR-9, PR-55 or PR-100 CD163 mutations failed to support a productive virus infection.

Finer mapping studies were performed by making additional PR insertions around the PR-55 mutation (see Figure 3.2B). A PR insertion placed just three amino acids downstream of PR-55 showed no effect on infection. However, a PR insertion placed after Val-47 reduced infection to levels similar to the PR-55 mutation (Table 3.5). Attempts were made to insert PR dipeptides between PR-48 and PR-55. However, no viable clones were obtained.

### **Effect of PR insertions on PRRSV-1 infection.**

In a previous study, we showed that pigs possessing a domain swap of SRCR5 for a homolog peptide sequence, SRCR8 from human-like CD163 were resistant to PRRSV-1, but not PRRSV-2 (Wells et al., 2017). The peptide sequences for SRCR5 and SRCR8 possess a difference of 31 amino acids, which are scattered throughout the polypeptide domain. In total, the results support the idea that PRRSV-1 and PRRSV-2 require SRCR5 but recognize different peptide in SRCR5 for infection. The experiment represented in Figure 3.2 was repeated using a PRRSV-1 isolate and the results summarized in Table 3.5. Only four of the 14 PR mutations produced the same results for PRRSV-1 and PRRSV-2. Of the mutations that produced the greatest effect on infection, there was only agreement for PR-100, which is located on the C-terminal end of the SRCR5 polypeptide.

**Effect of Glu to Lys substitution at position 58 (E58K) of SRCR5.** The results in Table 3.5 show that the PR-58 insertion had no effect on PRRSV-2 infection, but a dramatic impact on infection with the PRRSV-1 isolate. This observation is similar to the effect of the domain switch

of SRCR5 for hCD163L1 SRCR8. A comparison of the SRCR5 and SRCR8 peptide sequence shows a glutamic acid at position 58. Therefore, we hypothesized that Glu-58 was involved in the resistance of SRCR8 to infection with PRRSV-1. As shown in Figure 3.5A, HEK cells transfected with the mutated receptor or WT CD163 showed successful transfection at 48 hrs. In order to demonstrate the importance of E58K, we carried out PRRSV-1 and PRRSV-2 infection assays. At 2 days post-infection, cells were stained with PRRSV N-protein-specific mAb and Alexa Fluor 594-labeled anti-mouse IgG and visualized under a fluorescence microscope. Similar to the WT, the E58K mutated receptor showed the same level of PRRSV-2 infection (Figure 3.5A). In contrast, when probed for infection with PRRSV-1, the mutation resulted in a lower level of infection (Figure 3.5A). Overall, the E58K receptor showed a 64.9% decrease in permissiveness to PRRSV-1 (Figure 3.5B). These results are based on three independent experiments.

### **Orientation of PR insertions within the SRCR5 and effect on secondary and tertiary structures.**

Based on the X-ray crystallographic structure of porcine CD163 SRCR5, reported in Ma et al. (2016), we prepared a computer model of the predicted locations of the PR insertion locations on SRCR5. Figure 3.6B shows the location and effect of each PR insertion on PRRSV-2 infection. Even though the peptide sequence in Figure 3.2A shows that the PR-48 and PR-100 insertions are separated by 52 amino acids, they are brought together in close proximity within the 3-D model structure. The PR-9 and PR-55 mutations are also located within the same proximity, as are the PR-48 and PR-100 mutations. Based on the data in Table 3.5, it was expected that the pattern of mutations affecting PRRSV-1 infection would be different from

PRRSV-2. As illustrated in Figure 3.6A, the two mutations having the greatest effect on infection, PR-58 and PR-100, overlap with the general region occupied by the PR-9-48-55-100 mutations shown in Figure 3.6B. The location of the mutations placed on a surface model of SRCR5 is illustrated in Figure 3.7. The locations for the different PR mutations associated with PRRSV-1 or PRRSV-2 are located on the same face of the SRCR5 polypeptide.

The rationale for making the dipeptide PR insertions was the opportunity to affect PRRSV interaction by making localized disruptions in secondary structure. Ribbon models showing the predicted effect of each PR insertion are illustrated in Figure 3.8 and summarized in Table 3.6. The PR-100 mutation, which affects infection of transfected HEK cells by PRRSV-1 and PRRSV-2 isolates show no visible alteration of the SRCR5 structure.

## **SUMMARY AND CONCLUSIONS**

Genetically modified pigs lacking only CD163 SRCR5 are completely resistant to infection with PRRSV-1 or PRRSV-2 isolates (Whitworth et al., 2016). However, a distinct difference between PRRSV-1 and PRRSV-2 is found in how the SRCR5 domain is recognized (Wells et al., 2016). For example, alveolar macrophages from pigs possessing a domain swap between porcine CD163 SRCR5 and hCD163LI homolog SRCR8 support infection with PRRSV-2, but not PRRSV-1 isolates. There are 31 amino acid differences between porcine CD163 SRCR5 and hCD163LI SRCR8. The only available information on specific amino acid residues involved in the recognition of SRCR5 by PRRSV was recently reported by Ma et al. (2016), who prepared six SRCR5 variants possessing substitutions of arginine or aspartic acid residues with alanine. The selection of amino acids for substitution was based on peptide sequence comparisons between SRCR5 and the other eight CD163 SRCR domains. The results

showed that a single arginine to alanine substitution at position 561, R561A, was sufficient to reduce infection of transfected PK-15 cells. However, infection was only reduced by a single log. It should be noted that human CD163-like SRCR8 possesses a naturally occurring histidine substitution at the same 561 position. Since macrophages and pigs possessing a SRCR5 swapped with a human SRCR8 are susceptible to infection with PRRSV-2 isolates (Wells et al., 2017), it is unlikely that the R561A mutation is important.

In the present study, the approach for identification of peptide sequences and structures in SRCR5 involved in recognition by PRRSV was the insertion of single PR dipeptides along the SRCR5 polypeptide sequence. One rationale for the insertion of a PR dipeptide is to produce significant, but localized interruptions of primary, secondary and tertiary protein structures. On first analysis, only the PR mutations PR-58 and PR-100 produced an impact on the PRRSV-1 infection (Table 3.5, Figure 3.6A). On the other hand, PR-9, PR-55, or PR-100 produced the greatest impact on the PRRSV-2 infection of CD163-transfected HEK cells (see Table 3.5, Figures 3.2A and 3.6B). Finer mapping within the PR-55 region identified a fourth mutation, PR-48, which had a similar effect on PRRSV-2 infection (Figure 3.2B). Even though the relevant PR insertions are scattered throughout the SRCR5 peptide sequence, they come together within the folded protein (Figure 3.6B). The four mutations do not localize to ligand-binding pocket or CD6 loop 5-6 structure domains, which were previously described as putative PRRSV-binding sites (see Figure 3.2A; Van Gorp et al, 2010; Graversen et al., 2002). The four PR mutations encompass a possible binding pocket consisting of a two anti-parallel  $\beta$  strands and two opposing loop structures. The PR insertions likely prevent the interaction between PRRSV and CD163, by disrupting the antiparallel  $\beta$  strand structure, or by creating kinks in the opposing loop structures (see Figure 3.8).

**Table 3.1. Primers for amplification of CD163 inter-domain constructs shown in Table 3.2. The underlined nucleotides identify restriction sites.**

Construct	Primer Sequence
B	F-AGCAC <u>CCGCGG</u> CCTGACGGGACATGTAGCC R-ACAAC <u>CCGCGG</u> TGAGCAGGTAATTTGGCTTCGT
C	F-ACAC <u>CCGCGG</u> CTGGTTGGAGGGGACATTCCC R-AACT <u>CCGCGG</u> TGCTGCGGCGGCTGAGCAGGTAATTTTG
D	F-ACAC <u>CCGCGG</u> CTGGTTGGAGGGGACATTCCC R-AACT <u>CCGCGG</u> TTTTGCGGCGGCTGAGCAGGTAATTTGGC
E	F-ACAC <u>CCGCGG</u> CTGGTTGGAGGGGACATTCCC R-AACT <u>CCGCGG</u> TGCAGCGTGGGCTGAGCAGGTAATTT
F	F-TCAGCCGCAAGGGCT <u>CCGCGG</u> CTGGTTGGAGGG R-AACCAG <u>CCGCGG</u> AGCCCTTGC GGCTGAGCAGGTAATTT
G	F-ACAC <u>CCGCGG</u> CTGGTTGGAGGGGACATTCCC R-AACT <u>CCGCGG</u> TTTCTGGCGGCTGAGCAGGTAATTTGGC
H	F-CACAGGAGG <u>CCGCGG</u> CTGGTTGGAGGGGACATTCCC R-AACCAG <u>CCGCGG</u> CCTCCTGTGGGCTGAGCAGGTAAT
I	F-GCCACAAGAA <u>CCGCGG</u> CTGGTTGGAGGGGACATTCCC R-TCCAACCAG <u>CCGCGG</u> TTTCTTGTGGGCTGAGCAGGTAAT
J	F-AAGAA <u>CCGCGG</u> CTGGTTGGAGGGGACATTCCCTGC R-AACCAG <u>CCGCGG</u> TTTCTTCTTGGCTGAGCAGGTAATTTTG
K	F-GGAA <u>CCGCGG</u> CTGGTTGGAGGGGACATTCCCT R-ACCAG <u>CCGCGG</u> TTTCTGTGATCTGAGCAGGTAATTT
L	F-CTAA <u>CCGCGG</u> CTGGTTGGAGGGGACATTCCCTGCT R-AACCAG <u>CCGCGG</u> TTTAGCCCTGTGGGCTGAGCAGGTAATT
M	F-AGGAA <u>CCGCGG</u> CTGGTTGGAGGGGACATTCCCT R-AACCAG <u>CCGCGG</u> TTTCTTAGCGTGGGCTGAGCAGGTAATT

**Table 3.2. Peptide sequence modifications in the SRCR4/5 that affect infection.**

Construct	Peptide Sequence			Infection*	
	SRCR4	Inter-domain	SRCR5	PRRSV-1	PRRSV-2
A	KITCS	<b>AHRK</b>	PRLVG	+++	+++
B	.....	----	.....	+	+/-
C	.....	. <b>AAA</b>	.....	+++	+/-
D	.....	. <b>AA.</b>	.....	+++	+/-
E	.....	. <b>AA</b>	.....	+++	+++
F	.....	. <b>A.A</b>	.....	+++	+/-
G	.....	. <b>A.</b>	.....	+	+++
H	.....	. <b>.R</b>	.....	+++	+++
I	.....	. <b>K.</b>	.....	+++	++
J	.....	. <b>KK.</b>	.....	+++	+/-
K	.....	<b>D...</b>	.....	+++	+++
L	.....	<b>AHRAK</b>	.....	+++	+/-
M	.....	<b>AHARK</b>	.....	+++	+

\*Key: +++, infection of multiple cells with foci containing clusters of infected cells; +, fewer number of infected cells, but still possessing foci containing clusters of infected cells; ++, several single cells infected with virus; + a small number of cells showing infection; +/- only one or two infected cells in the well.

**Table 3.3. Primer sequences for the preparation of SRCR5 mutations. SacII restriction sites are underlined.**

<b>Construct</b>	<b>Primer Sequence</b>
PR-9	F-ATTAC <u>CCGCGG</u> CCCTGCTCTGGTCTGTGTTG R-ATTAC <u>CCGCGG</u> AATGTCCCCTCCAACCAGCC
PR-15	F-CAC <u>CCCGCGG</u> GAAGTACAACATGGAGACACGTGGGG R-ACCAC <u>CCCGCGG</u> AACACGACCAGAGCAGGGGAATGTC
PR-22	F-ATTAC <u>CCGCGG</u> TGGGGCACCGTCTGTGATTC R-GTGAC <u>CCGCGG</u> CGTGTCTCCATGTTGTA <del>CTT</del> CAAC
PR-32	F-TATA <u>CCGCGG</u> CTGGAGGCGGCCAGCGT R-CGCT <u>CCGCGG</u> GAGAGAAGTCAGAATCACAGACGGTGC
PR-38	F-GATA <u>CCGCGG</u> CTGTGCAGGGA <del>ACT</del> TACAGTGCGGCACT R-TATA <u>CCGCGG</u> CACGCTGGCCGCCTCCAGAGAGAA
PR-42	F-AT <u>CCCCGCGG</u> CTACAGTGCGGCACTGTGGTTTCC R-ATCA <u>CCGCGG</u> TTCCTGCACAGCACGCTGGC
PR-44	F-CACAC <u>CCGCGG</u> TGCGGCACTGTGGTTTCC R-TA <u>ACCCGCGG</u> CTGTAGTTCCTGCACAGCACG
PR-48	F-CACAC <u>CCGCGG</u> GTTTCCCTCCTGGG R-CCCAC <u>CCGCGG</u> CACAGTGCCGCACTGTAG
PR-55	F-CA <u>ACCCGCGG</u> CACTTTGGAGAAGGAAGTGGACAGATCTGGGC R-ACA <u>CCCGCGG</u> GAGCTCCCCCAGGAGGGAAACCAC
PR-58	F-CA <u>ACCCGCGG</u> GAAGGAAGTGGACAGATCTGGGCTGAAGA R-ATTAC <u>CCGCGG</u> TCCAAAGTGAGCTCCCCCAGGA
PR-62	F-CA <u>ACCCGCGG</u> CAGATCTGGGCTGAAGAATTCCAGTGT R-CACAC <u>CCGCGG</u> TCCACTTCCTTCTCCAAAGTGAGCTCCC
PR-67	F-CAC <u>CCCGCGG</u> GAATTCCAGTGTGAGGGGCACGAG R-AC <u>CCCCGCGG</u> TTCAGCCAGATCTGTCCACTTCC
PR-78	F-AAGG <u>CCGCGG</u> TCACTCTGCCAGTAGCACCCC R-CACAC <u>CCGCGG</u> AAGGTGGGACTCGTGCCCTCACA
PR-89	F-CCGAC <u>CCGCGG</u> ACATGTAGCCACAGCAGGGACGTC R-TATA <u>CCGCGG</u> CCCGTCAGGGCGGGGTGC
PR-100	F-CGCG <u>CCGCGG</u> TGCTCAAGATACACAAATCCGC R-CA <u>ACCCGCGG</u> GACTACGCCGACGTCCCTGC

**Table 3.4. Percent infection of HEK293T cells transfected with different PR dipeptide insertion constructs\*.**

	<b>Exp. 1</b>	<b>Exp. 2</b>	<b>Exp. 3</b>	<b>Mean+/- SD</b>
<b>10<sup>-1</sup> Dilution of Virus</b>				
<b>WT</b>	55.3	62.3	60.4	59.3+/-3.6
<b>PR-9</b>	2.1	3.0	1.6	2.2+/-0.7
<b>PR-55</b>	1.7	1.6	1.4	1.6+/-0.2
<b>PR-100</b>	0.8	1.1	1.2	1.0+/-0.2
<b>10<sup>-2</sup> Dilution of Virus</b>				
<b>WT</b>	28.5	28.5	30.6	29.2+/-1.2
<b>PR-9</b>	0.7	1.0	0.6	0.8+/-0.2
<b>PR-55</b>	0.0	0.0	0.0	0
<b>PR-100</b>	0.4	0.5	0.4	0.4+/-0.1
<b>10<sup>-3</sup> Dilution of Virus</b>				
<b>WT</b>	3.2	4.5	6.6	4.8+/-1.7
<b>PR-9</b>	0	0	0	0
<b>PR-100</b>	0	0	0	0
<b>10<sup>-4</sup> Dilution of Virus</b>				
<b>WT</b>	0	1.3	1.4	0.9+/-0.8
<b>10<sup>-5</sup> Dilution of Virus</b>				
<b>WT</b>	0	0	0	0

\*Cells were infected with different dilutions of P129-RFP virus (starting concentration = 6.5 log<sub>10</sub>TCID<sub>50</sub>/ml). Results are shown as percent infection of CD163-positive HEK293T cells at 72 hrs after infection. Each experiment was performed on a single 24-well plate. Transfection efficiency, as determined by the percentage of green fluorescent cells for the CD163-EGFP plasmid constructs was between 60 and 70% (data not shown).

**Table 3.5. Comparison of infection results for PRRSV-1 and PRRSV-2\*.**

<b>Mutation</b>	<b>Infection results</b>	
	<b>PRRSV-1</b>	<b>PRRSV-2</b>
PR-9	+++	+/-
PR-15	+++	+++
PR-22	+++	+
PR-32	+	+
PR-38	++	+++
PR-42	+++	+++
PR-48	+++	+/-
PR-55	+++	+/-
PR-58	+/-	+++
PR-62	++	++
PR-67	+++	+
PR-78	+++	+++
PR-89	+	++
PR-100	+/-	+/-

\*Gray shaded rows show viruses with the same infection results. The key for results is the same as described in Figure 3.2.

**Table 3.6. Effect of PR insertions on secondary structure of SRCR5\*.**

<b>Name</b>	<b>Mutation</b>	<b>Effect on 2<sup>nd</sup> Structure</b>
PR-9	8-Iso- <b>Pro-Arg</b> -Pro	No effect on 2 <sup>nd</sup> structure
PR-48	47-Val- <b>Pro-Arg</b> -Val	Truncation of $\beta$ 4
PR-55	54-Ala- <b>Pro-Arg</b> -His	Disappearance of $\beta$ 4
PR-58	57-Glu- <b>Pro-Arg</b> -Gly	Disappearance of $\beta$ 4
PR-100	100-Val- <b>Pro-Arg</b> -Cys	Truncation of $\beta$ 7

\*The results are based on the structures illustrated in Figure 3.8. The PR insertion is shown in bold for each mutation.

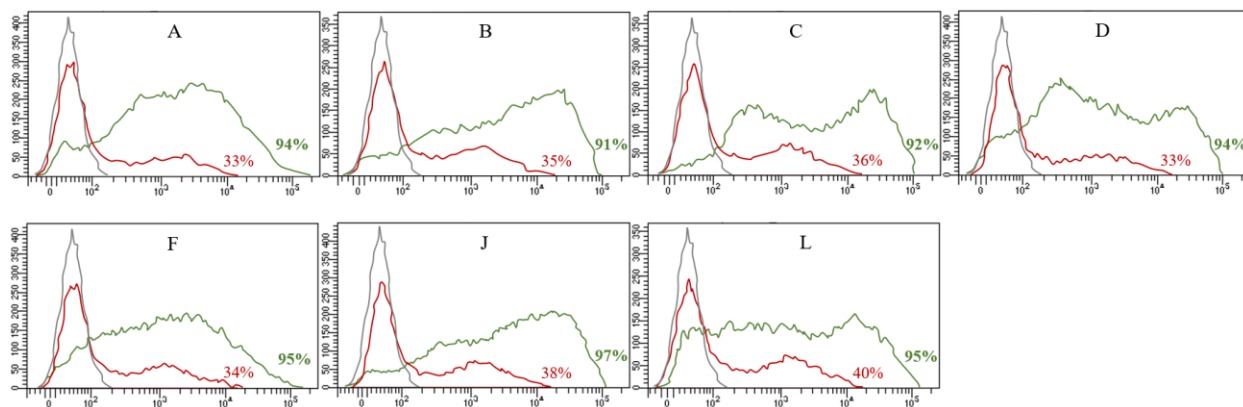


**Figure 3.1. Surface expression of CD163 interdomain constructs expressed in transfected HEK cells.** Letters refer to the constructs shown in Table 3.2. Surface expression of CD163 constructs expressed in HEK cells. The histograms show the GFP expression green, the mAb 2A10 staining in red and the isotype control in gray. Cells were stained 48 hrs after transfection. The mAb 2A10 staining results are shown as percentage of CD163-positive cells from the GFP-positive gated population.



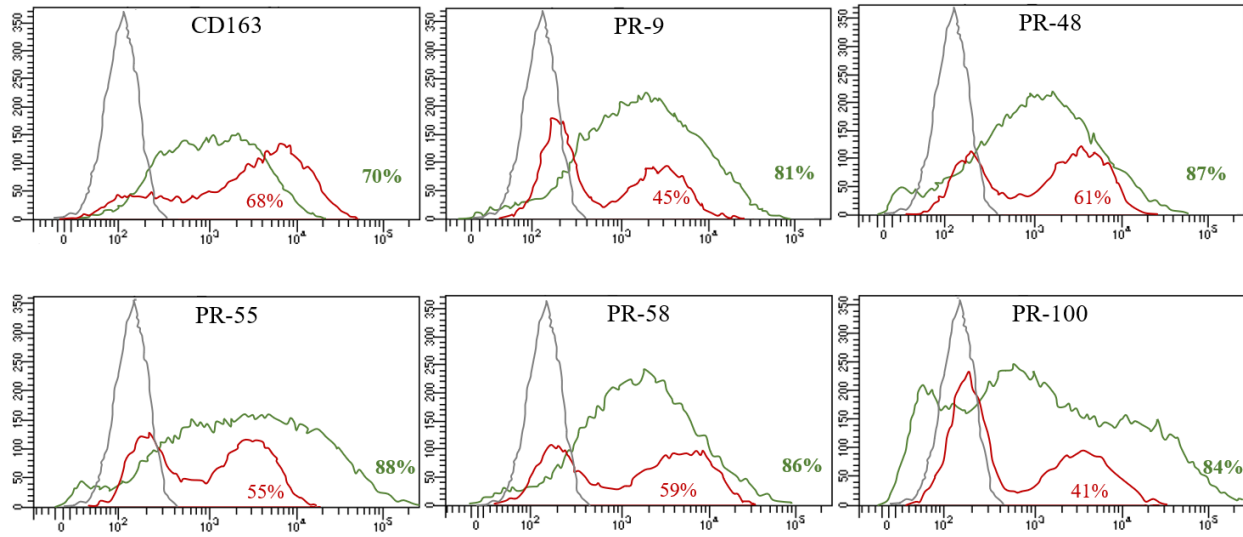


**Figure 3.3. Surface expression of SRCR5 PR insertion constructs expressed in HEK cells.** The histograms show the GFP expression green, the mAb 2A10 staining in red and the isotype control in gray. Cells were stained 48 hrs after transfection. The mAb 2A10 staining results are shown as percentage of CD163-positive cells from the GFP-positive gated population.

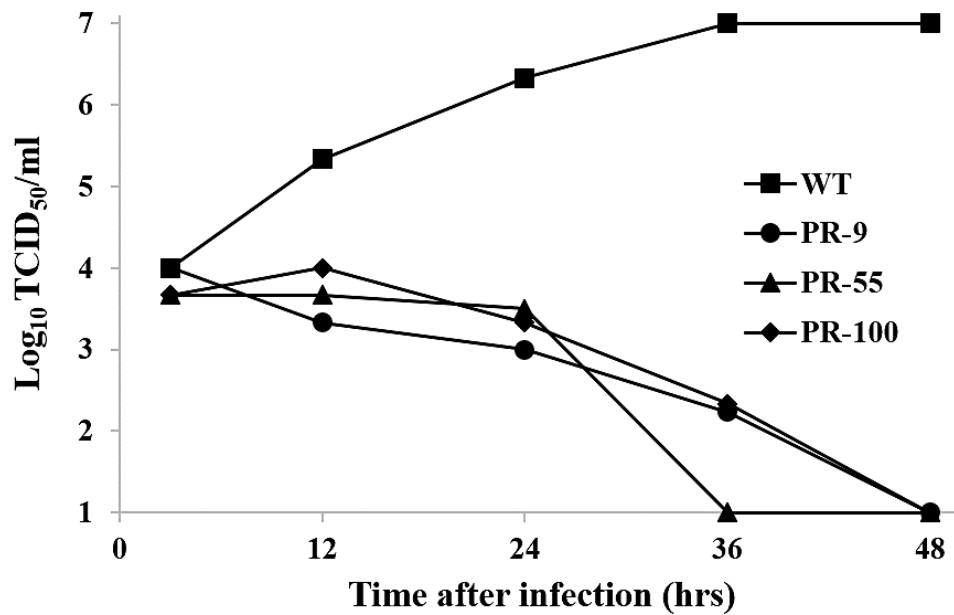


**Figure 3.4. Growth curves for HEK293T cells transfected with wild-type and mutant CD163 constructs.** HEK cells transfected with different mutant constructs and after 24 hrs infected with PRRSV P129-RFP. Two hours post-infection, the cells were washed, and media was collected every 12 hrs. The TCID<sub>50</sub> was calculated by titration of viruses on MARC-145 cells. Results are shown for a single experiment.

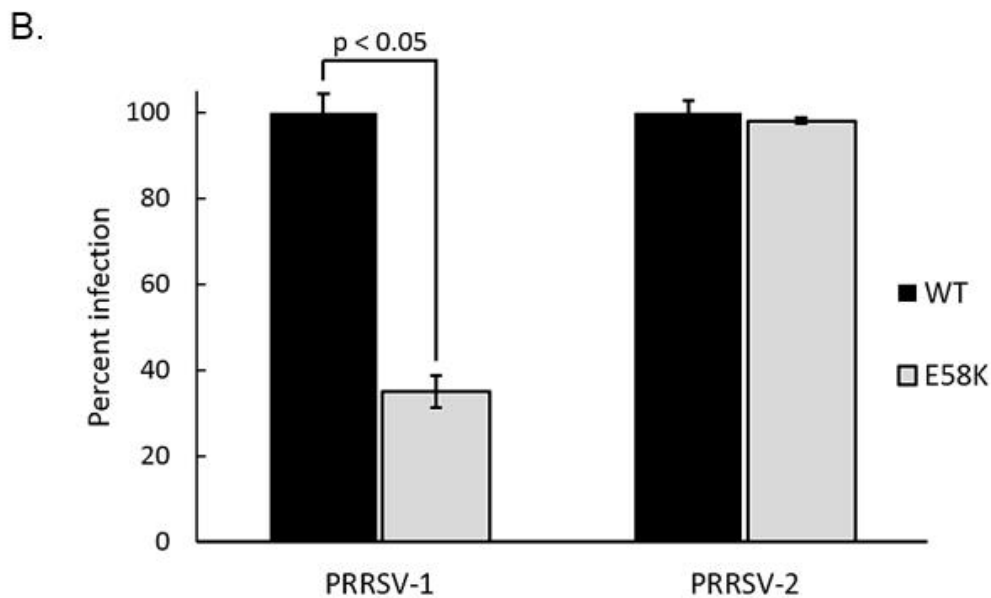
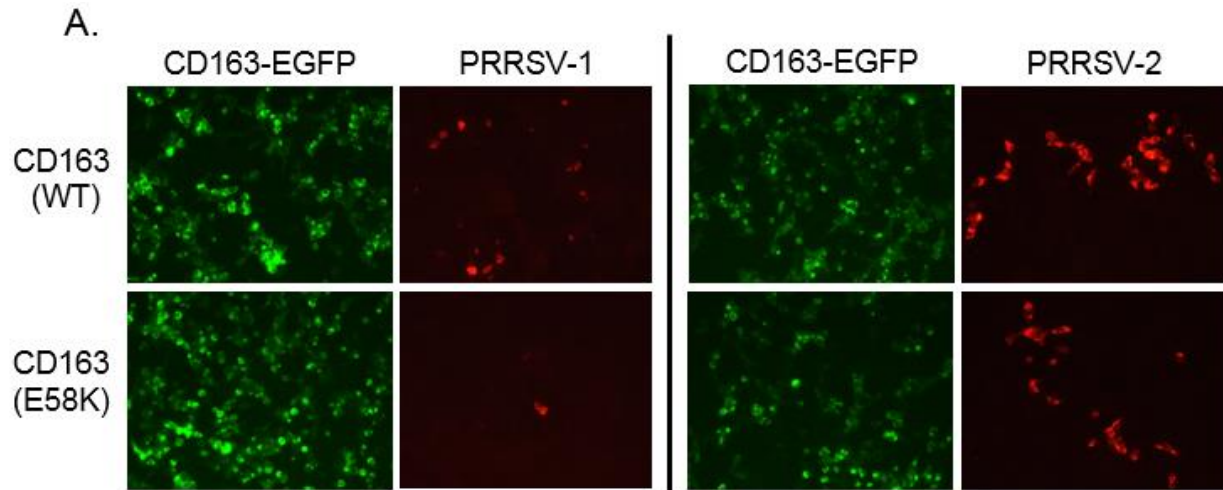
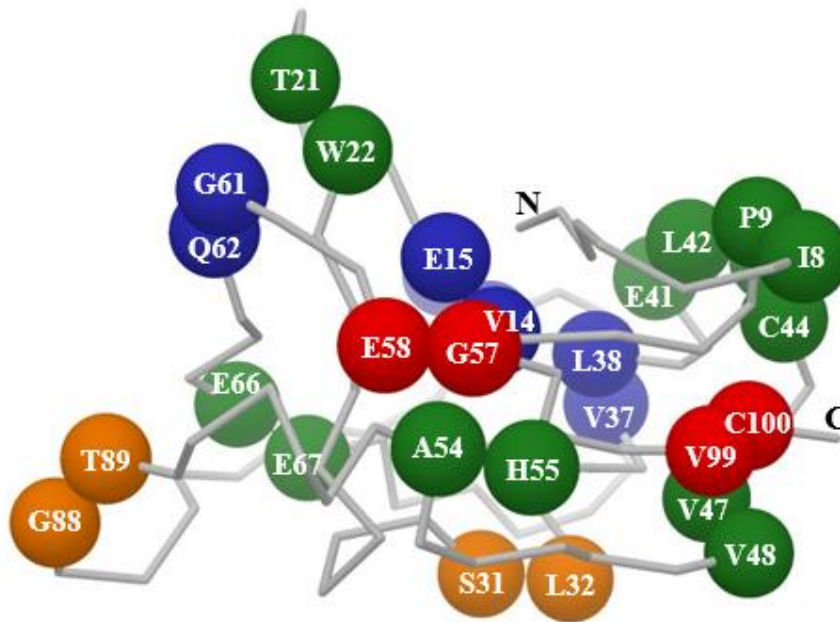


**Figure 3.5. Effect of Glu to Lys substitution at position 58 (E58K) of SRCR5.** (A) Non-permissive HEK cells were transfected with either E58K mutation or WT CD163 (represented in green). At 24-48 hrs post-transfection, the cells were infected with PRRSV-1 at a MOI of 0.1 and with PRRSV-2 with a MOI of 1. Following staining against the PRRSV N-protein (represented in red), a positive result for infection was recorded as a cell expressing both green and red fluorescence. (B) The infection on HEK cells transfected with the E58K mutation was measured as percent of PRRSV positive cells. Data represents means from three independent experiments. A  $p < 0.05$  indicates significantly reduced level of infection for PRRSV-1.

A. PRRSV-1



B. PRRSV-2

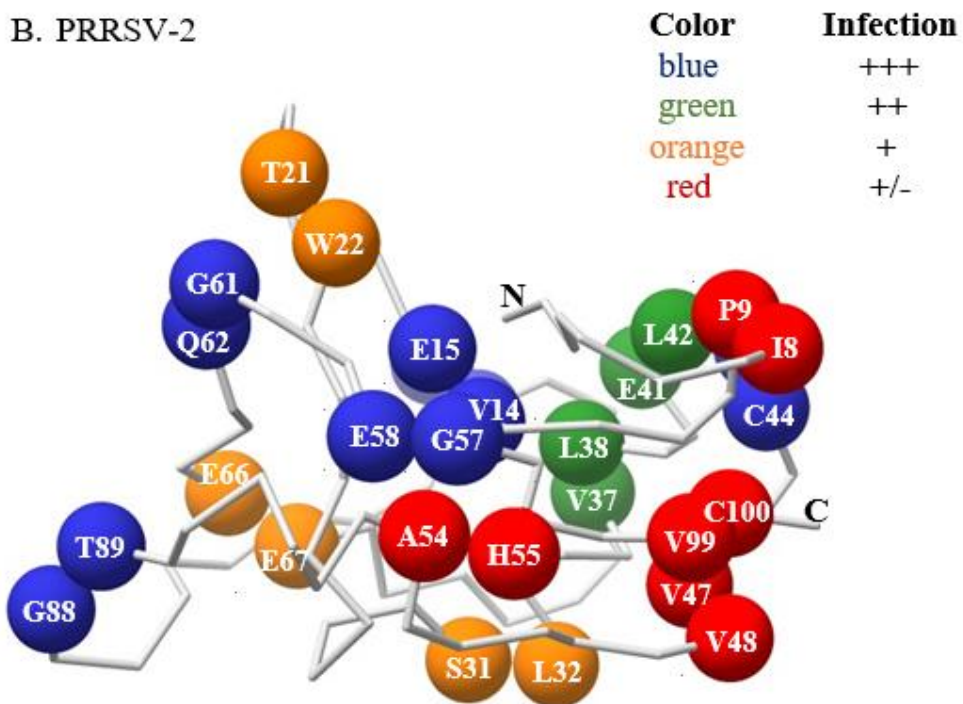


**Figure 3.6. Predicted location and of PR insertions in SRCR5.** Each amino acid pair in the ribbon structure identifies the location of each PR insertion. The structures are based on the X-ray crystallography data deposited in RCSB Protein Data Bank (PDB code 5JFB) and viewed using UCSF Chimera (Pettersen et al., 2004). The key for the infection rate for each mutation is described in Figure 3.2.

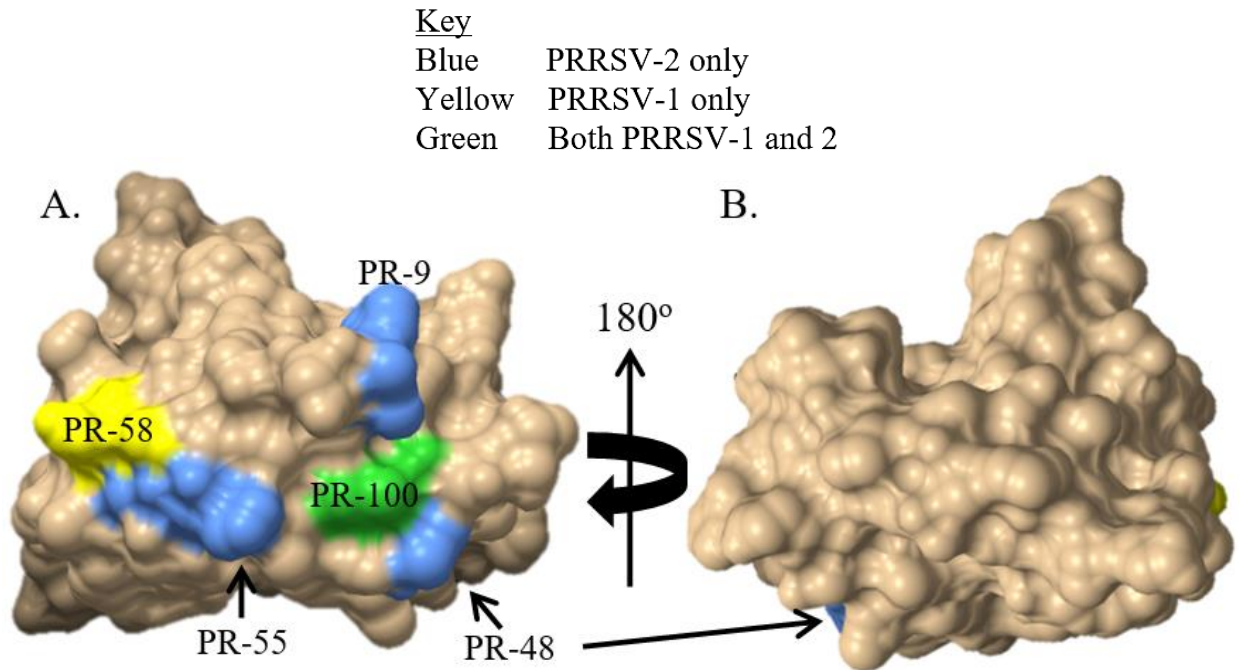


**Figure 3.7. Surface location of mutations in SRCR5 that affect PRRSV-1 and PRRSV-2 infection.** The figure is a surface model showing the location of the PR insertions in color. Each colored region represents the same dipeptides shown in Figure 3.2. Orientation A shows all mutation sites. Orientation B shows a 180° rotation of the polypeptide.

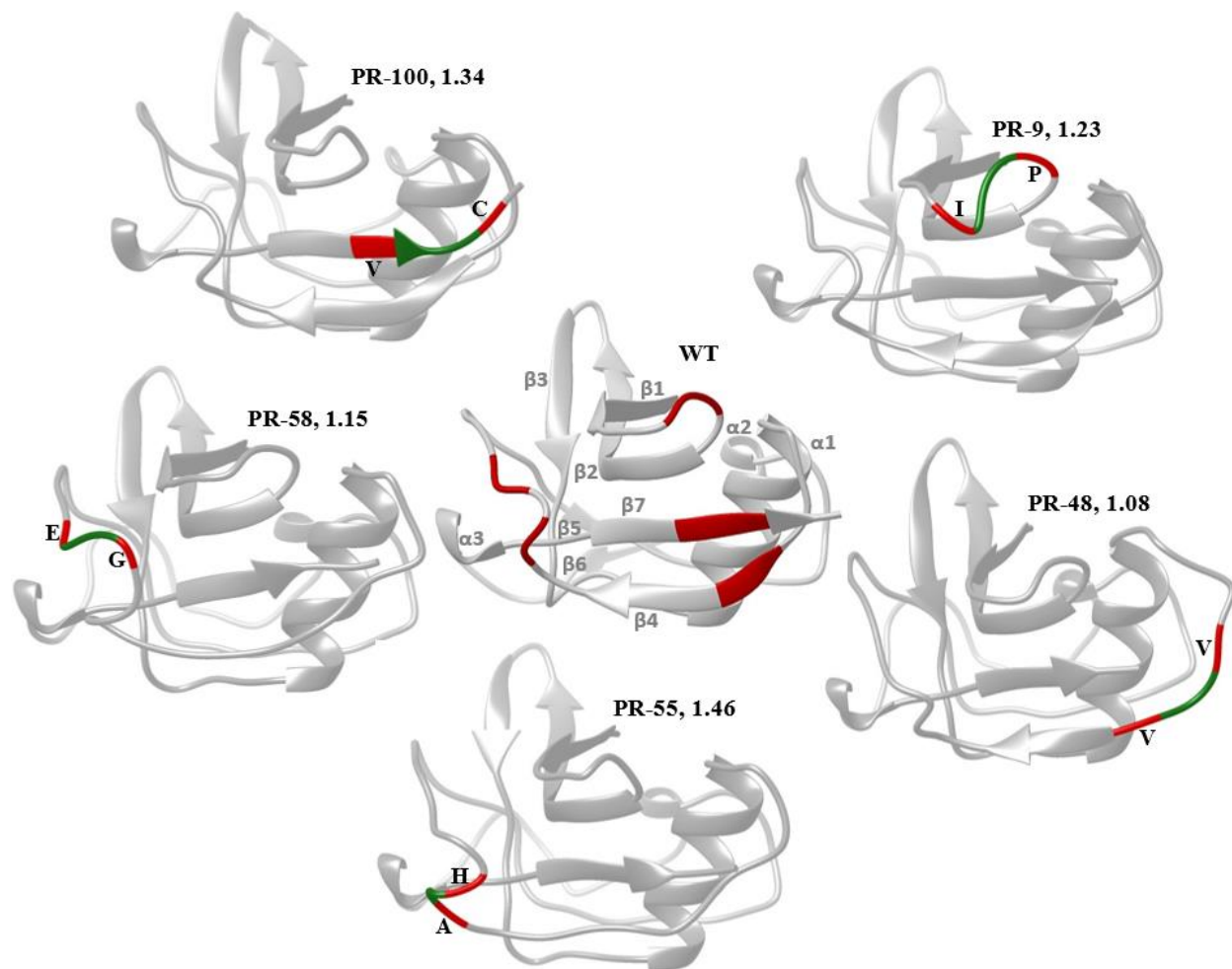


**Figure 3.8. Predicted effects of PR insertions on the secondary structure of SRCR5.** The ribbon model structures were computer-generated using the same modeling software described in Figure 3.6. The mutation name and C-value are shown for each structure. Red shows the location for each insertion and the green represents the PR dipeptide. The wild-type structure is in the middle.

# **Chapter 4 - Characterization of monoclonal antibody 2A10 against different porcine CD163 deletion constructs**

## **INTRODUCTION**

Several antibodies against the CD163 protein have been generated as useful tools in studying its function or involvement in different processes. The monoclonal antibody (mAb) 2A10 was produced by immunizing pigs with porcine alveolar macrophages (Bullido et al., 1997) and was shown to recognize the porcine CD163 expressed on cells of the monocyte/macrophage lineage (Sanchez et al., 1999). Since then, the antibody has been used extensively as a marker for differentiated macrophages, for confirming the presence or absence of CD163 expression in different edited cell lines or pigs (Burkard et al., 2017; Wells et al., 2017) and to block PRRSV infection *in vitro* (Van Gorp et al., 2008; Van Gorp et al., 2010). Nonetheless, these previous studies that used CD163 deletion constructs showed that in some edits, the mAb 2A10 fails to react with the recombinant proteins. Our hypothesis is that the CD163 antibody recognizes an epitope that was deleted from those constructs. Therefore, the purpose of this study is to identify the localization of the 2A10 epitope by using the large number of CD163 deletion constructs that were previously generated.

## **MATERIALS AND METHODS**

**Preparation of the N-terminal deletion construct (construct B).** To prepare this recombinant N-terminal deletion construct, primers were designed with KpnI and XbaI restriction sites on the 5' and 3' ends, respectively. The primers used for amplification and cloning of the construct are

listed in Table 4.1. Wild-type CD163 cloned in pcDNA3.1-EGFP vector (construct A) provided by Dr. Dongwan Yoo (University of Illinois, College of Veterinary Medicine, USA) was used as a template. The fragment was amplified using the GoTaqGreen<sup>®</sup> Master Mix (Promega) according to manufacturer's instructions and a protocol as follows: 95 °C for 2 min, 30 cycles (94 °C for 30 s, 65 °C for 30 s, and 72 °C for 2 min), and 72 °C for 10 min. The PCR product was cloned into pCR<sup>®</sup>2.1-TOPO<sup>®</sup> vector (Invitrogen) according to manufacturer's instructions. The plasmid was transformed into One Shot<sup>®</sup> TOP10 chemically competent *E.coli* cells (Invitrogen), according to manufacturer's instructions. Several clones per sample were selected from the transformation plate and transferred into Luria-Bertani (LB) agar with 100 µg/ml of Ampicillin. Clones were screened by double digestion with KpnI and XbaI for the presence of the target insert. The successful clone was double-digested with KpnI (New England Biolabs Inc.) and XbaI (New England Biolabs Inc.) and cloned in frame into the KpnI-XbaI sites on the original pcDNA3.1-EGFP vector using a 1:3 ratio vector:insert. The new plasmid was transformed into One Shot<sup>®</sup> TOP10 chemically competent *E.coli* cells and three clones were checked for the in-frame deletion of SRCR1 by DNA sequencing.

**Preparation of the C-terminal deletion constructs (constructs C and D).** For these recombinant proteins, primers were designed with PacI restriction sites followed by an additional nucleotide that ensured the in-frame deletion (Table 4.1). As described above, wild-type CD163 in pcDNA3.1-EGFP vector (construct A) was used as a template. For this PCR we used the LongAmp<sup>®</sup> *Taq* DNA Polymerase (New England Biolabs Inc.) with a protocol as follows: 94 °C for 30 s, 30 cycles (94 °C for 30 s, 65 °C for 1 min, and 65 °C for 8 min), and 65 °C for 10 min. The PCR products were digested with PacI and religated using Anza<sup>™</sup> T4 DNA Ligase Master

Mix (Invitrogen) according to manufacturer's instructions and transformed into One Shot<sup>®</sup> TOP10 chemically competent *E.coli* cells. Based on restriction endonuclease enzyme analysis and DNA sequencing, *E. coli* colonies harboring plasmids with correct deletions were selected.

**Transfection of HEK293T (HEK) cells.** Constructs A through D were transfected into HEK cells using FuGENE<sup>®</sup> HD reagent (Promega) according to manufacturer's instructions. Briefly, HEK cells were plated at a density of  $8 \times 10^4$  cells on a 24-well plate. After 24 hrs, when the cells were 80-90% confluent, the mixtures of transfection reagent and plasmid were added into the cell culture at a 3:1 ratio. At 24-48 hrs post-transfection, the cells were examined for the presence of EGFP expression under a fluorescence microscope (Nikon ECLIPSE TE2000-S) and stained by immunofluorescence antibody (IFA) assay or analyzed by flow cytometry and western blot.

**Western blot analysis on transfected cells.** Cell monolayers were washed once with cold PBS, re-suspended in NP-40 lysis buffer (Invitrogen) and detached using cell scrapers. The detached cells were placed on ice in 1.5 mL Eppendorf tubes for 30 min under constant agitation. Lysates were centrifuged and the supernatants were loaded immediately into wells of 10% SDS-PAGE gels at 150V for 45 minutes, according to manufacturer's instructions (Invitrogen). The proteins were blotted onto 0.45  $\mu$ m PVDF membranes (Amersham), blocked using 5% non-fat dry milk in PBS (NFDm) and incubated for 1 hr at room temperature (RT). Following the blocking step, the membranes were washed with PBS-Tween20 and incubated with either horseradish peroxidase (HRP)-conjugated goat anti-GFP antibody (R&D Systems), diluted 1:1000 in PBS-NFDm or with mouse anti-porcine CD163 mAb (Clone: 2A10/11, BIO-RAD), diluted 1:500 in

NFDM, followed by an incubation with HRP-conjugated goat anti-mouse IgG antibody (KPL; 1:3000 dilution). After 1 hr of incubation at RT, the reaction was visualized using the CN/DAB Substrate Kit (Thermo Scientific Pierce) by adding the substrate to the membrane and incubating it for 5 to 10 minutes at RT until color developed. The reaction was stopped by rinsing the membrane with double-distilled water. A picture of the membrane was acquired using the UVP GelDoc-It™ Imaging System. The membranes stained with the anti-CD163 antibody were run under non-reducing conditions.

**Indirect immunofluorescence assay on transfected cells.** Forty-eight hours post-transfection with the recombinant proteins, HEK cells were washed three times with PBS and fixed with 4% paraformaldehyde (Thermofisher Scientific) for 10 min at RT and permeabilized with 0.1% Triton-X for 5 min at RT. The cells were then incubated with mouse anti-porcine CD163 mAb (Clone: 2A10/11, BIO-RAD), 1:200 dilution in PBS, for 1 hr at 37 °C. After three washes with PBS, the cells were incubated with Alexa Fluor 594-conjugated goat anti-mouse IgG (H+L) antibody (Thermofisher Scientific), diluted 1:400 in PBS, for 1 h at 37°C. The cells were counterstained with DAPI for 5 min at RT, washed three times with PBS and examined under the fluorescence microscope.

**Measurement of surface expression by flow cytometry.** Forty-eight hours post-transfection, cells were washed twice with PBS and detached with TrypLE™ Express (Thermofisher Scientific). Approximately  $2 \times 10^7$ /mL cells were re-suspended in an appropriate volume of PBS with 10% mouse serum (PBS-MS) and incubated for 15 min at 4 °C. Cells were pelleted by centrifugation and re-suspended in 100 µl of R-Phycoerythrin (RPE) conjugated mouse anti-

porcine CD163 mAb (Clone: 2A10/11, BIO-RAD). After a 30 minutes incubation the cells were washed twice with 2% PBS-MS and brought to a final volume of 300-500  $\mu$ l and analyzed on the BD LSR Fortessa X-20 Flow Cytometer (BD Biosciences) with FCS Express 5 software (De Novo Software). A minimum of 10,000 cells were analyzed for each sample. GFP-only and RPE-only samples along with an isotype control consisting of HEK cells stained with an RPE-conjugated mouse IgG1 negative control (BIO-RAD) were included in the experiment.

**Production of recombinant SRCR1 in *E. coli*.** The porcine CD163 sequence (GenBank Acc No. EU016226) was used for the preparation of the SRCR1 recombinant protein. The corresponding nucleotide sequence was codon optimized for expression in *E. coli* and synthesized by Integrated DNA Technologies (IDT). SacII and EcoRI restriction sites were incorporated into the 5' and 3' ends of the synthesized fragment. The SRCR1 domain was cloned into a pHUE bacterial expression vector which expresses a 6xHis ubiquitin fusion protein (Catanzariti et al., 2004). The plasmid was transformed into *E. coli* BL21 (DE3) competent cells (New England Biolabs) and the successful cloning of the SRCR1 domain was confirmed by DNA sequencing. For the purpose of recombinant protein expression, BL21 cells containing the pHUE plasmid and the SRCR1 protein, were grown in LB media at 37 °C until the optical density (OD600) reached the 0.4-0.6 range. Protein expression was induced by the addition of Isopropyl  $\beta$ -D-1-thiogalactopyranoside (IPTG) to a final concentration of 0.1 mM. After addition of IPTG, the bacterial cells were grown for an additional 4 hours and then harvested by centrifugation 4000 x g for 10 minutes. Aliquots of 1 ml were taken at 0 hr and 4 hrs after the addition of IPTG. The aliquots were pelleted and suspended in 100  $\mu$ l of SDS sample buffer (sodium dodecyl sulfate with Tris-HCl pH 6.8, glycerol,  $\beta$ -mercaptoethanol,

ethylenediaminetetraacetic acid (EDTA) and bromophenol blue) for analysis by SDS-PAGE. The recombinant protein was purified from the bacterial pellet using PrepEase His-Tagged Protein Purification Kit (USB), using a protocol incorporating 0.3% Sarkosyl and 0.5 M CAPS buffer. Affinity purification was performed on a nickel column that captures the 6x His-tagged protein and the purity assessed by SDS-PAGE. Specificity of the recombinant protein was verified by western blot as described above using either an anti-His tag mAb (Clone J099B12; Biolegend; 1:1000 dilution) or the anti-CD163 mAb (Clone 2A10; 1:500 dilution), followed by incubation with an HRP-conjugated goat anti-mouse IgG (KPL; 1:3000 dilution). The results were visualized using the CN/DAB Substrate Kit (Thermo Scientific Pierce) by adding the substrate to the membrane and incubation at room temperature until the color developed. The reaction was stopped by rinsing the membrane with double-distilled water. A picture of the membrane was acquired using the UVP GelDoc-It™ Imaging System.

## RESULTS

### **Reactivity of anti-CD163 monoclonal antibody in HEK cells transfected with different CD163 constructs.**

The reactivity of the mAb 2A10 was first assessed by western blot, IFA and flow cytometry against different CD163 deletion constructs that were transfected into HEK cells. This approach was used for identification of the region recognized by the mAb 2A10. The different CD163 deletion constructs used in this study are represented in Figure 4.1A. As shown in Figures 4.1B and 4.1C, at 48 hrs post-transfection, the HEK cells expressing CD163 constructs fused to enhanced green fluorescent protein (EGFP) were analyzed by western blot using either an anti-GFP Ab (see Figure 4.1B) or the mAb 2A10 (see Figure 4.1C). When detected using the

anti-GFP Ab, all constructs (A through D) resulted in a band of the predicted molecular weight (Figure 4.1B) whereas, only constructs A, C and D reacted positively when tested on a western blot against the mAb 2A10 (Figure 4.1C). The result suggests that the anti-CD163 mAb 2A10 recognizes an epitope within CD163 SRCR1 under non-reducing conditions. This seems to be in accordance with the results from the IFA and flow cytometry assays on the HEK cells transfected with different CD163 constructs. As shown in Figures 4.2 and 4.3, the anti-CD163 mAb failed to recognize construct B, whereas constructs C and D were recognized at a similar level compared to the WT CD163 (construct A). Taken together, these data show that the negative result seen in construct B comes from the lack of specificity of the antibody against SRCR1, rather than from a conformational change and therefore absence of recognition.

#### **Specificity of mAb 2A10 against SRCR1 recombinant protein.**

In order to confirm the results from the first experiments, SRCR1 from the porcine CD163 was cloned in a pHUE expression vector. This *E. coli* expression vector was used because of its 6x histidine tag and ubiquitin; the His tag allows for simple affinity column purification and the fusion of cloned proteins to ubiquitin increases the bacterial expression and solubility of the peptides. The expression and purification of the SRCR1 recombinant protein resulted in a band of the predicted molecular weight (Figure 4.4A). The purified protein also reacted positively when tested on a western blot against the anti-histidine antibody, confirming the successful cloning in the pHUE vector (Figure 4.4B). Using the purified SRCR1 recombinant protein, the mAb was also tested for its reactivity on a western blot. As shown in Figure 4.4C, the antibody specifically detected a protein band just above the 10 kDa protein marker, which corresponds to the predicted size of the recombinant protein.

## SUMMARY AND CONCLUSIONS

There is currently no information regarding the location of the epitope recognized by the commercial anti-CD163 mAb (Clone 2A10). Based on their limited CD163 deletion constructs, Van Gorp et al. (2010) showed that the epitope recognized by this antibody is present in one of the first three N-terminal domains but failed to point to a more accurate location. The approach used in our study relies on the systematic deletion of individual SRCR domains in CD163 that allows for a more accurate localization of the epitope. We successfully generated different constructs (see Figure 4.1A) that we transfected in HEK cells which do not express CD163; according to the western blot, IFA and flow cytometry data (see Figures 4.1-4.3), this system allowed us to identify SRCR1 domain as the region recognized by the anti-CD163 antibody. Furthermore, in order to confirm the specificity of the antibody for the first N-terminal domain of CD163, we cloned this region in a pHUE vector and expressed it in a bacterial system. As shown in Figure 4.4, the mAb 2A10 recognized the SRCR1 recombinant protein under non-reducing conditions. This result explains the inability of the anti-CD163 antibody to block PRRSV infection (Van Gorp et al., 2010), as PRRSV has been shown to interact with CD163 SRCR5, not SRCR1. Nonetheless, future studies are needed in order to identify the exact epitope within SRCR1 that the antibody recognizes.

**Table 4.1. Primers for amplification of CD163 deletion constructs shown in Figure 4.1. The underlined nucleotides identify restriction sites.**

<b>Construct</b>	<b>Primer Sequence</b>
B	F- <u>GGTACCAT</u> GGGATCTGATTTAGAGATGAGG R- <u>TCTAGATT</u> GTA <del>CTTCAGAGTGGTCTCC</del>
C	F-ATTATTA <u>AATTAAG</u> TTTGTGCACTTGCAATCTTTGGGGT R-ATC <u>ATTAATTA</u> AATTTAAGCAAATCACTCCAGCATCCTCAG
D	F- <u>ACTGCCGCGG</u> CACAGTGGCGGCCGCTCGAGTCTAGAATG R-ATC <u>GCCGCGG</u> GTACCAAGCTTAACTAGCCAGCTTGGGTCTCCC

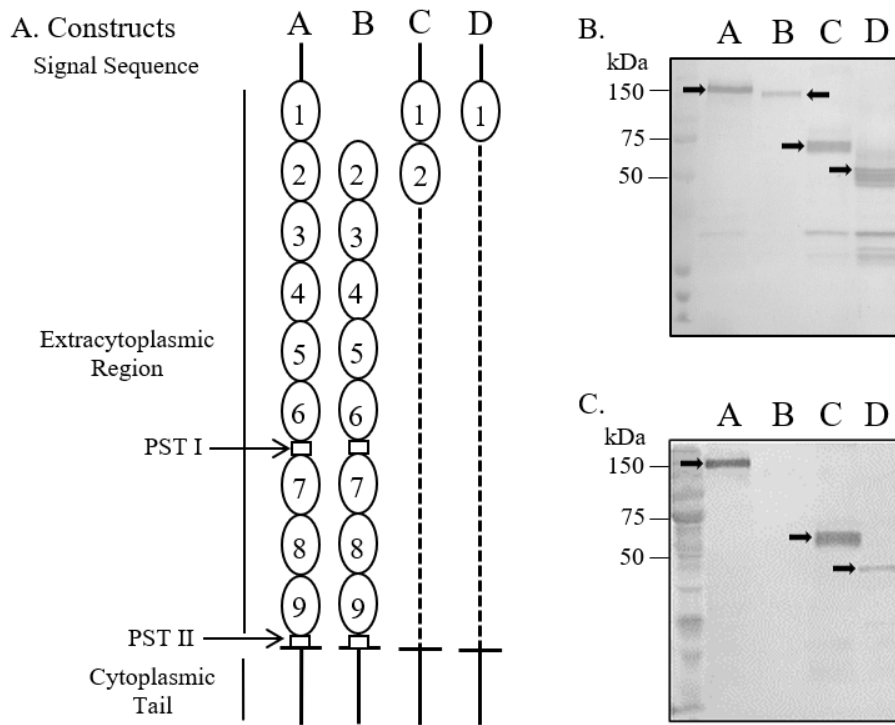


**Figure 4.1. CD163 constructs used to characterize the CD163 mAb 2A10.** (A) Deletion mutants used in the transfection of HEK cells. Ovals and squares identify the SRCR and PST domains, respectively. (B) Result for western blot using anti-GFP antibody for the detection of the CD163-EGFP fusion protein. (C) Results for western blot using the anti-CD163 mAb 2A10.

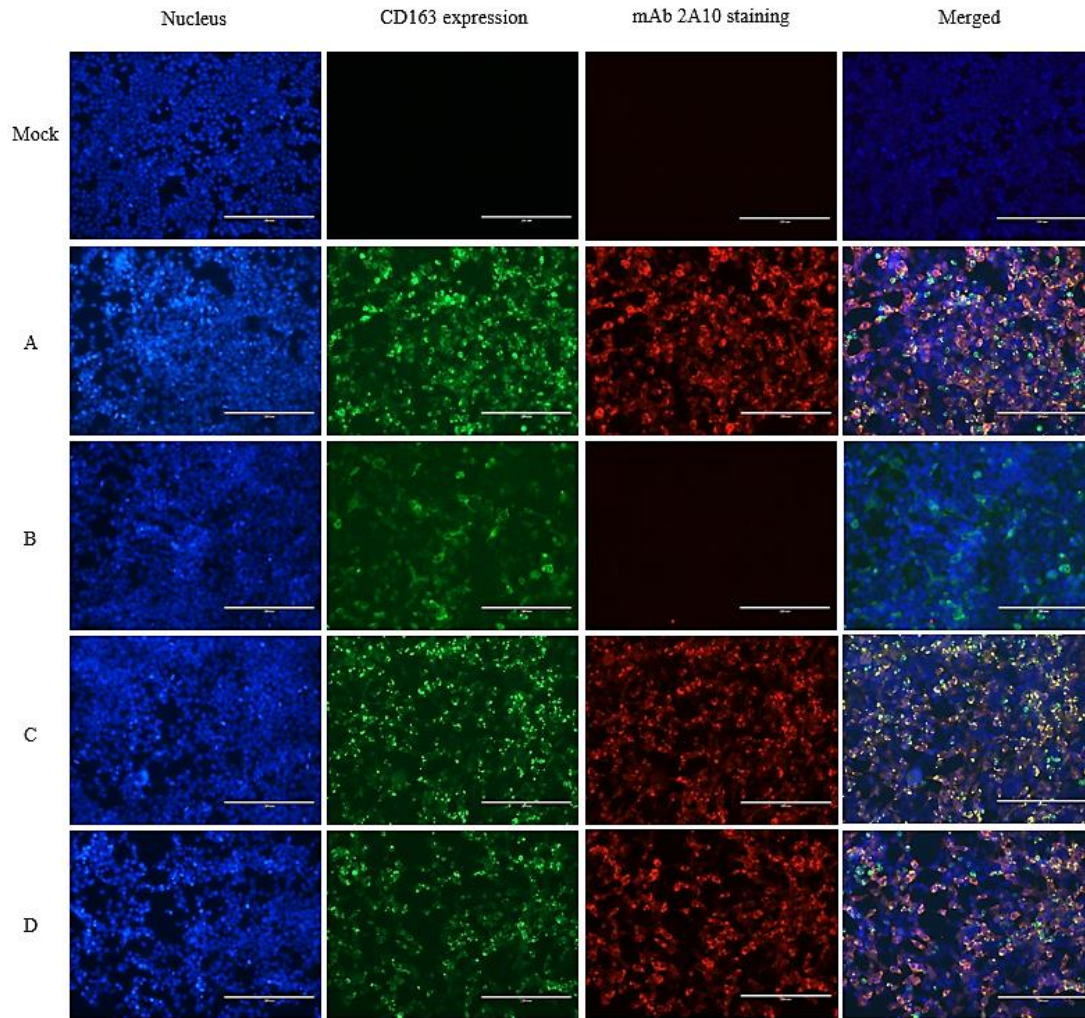


**Figure 4.2. Detection of CD163 expression in transfected HEK cells by immunofluorescence antibody assay using the mAb 2A10.** HEK cells were transfected with different CD163 deletion constructs and after 48 hrs were visualized under the fluorescence microscope for GFP expression (green); the transfected cells were fixed and incubated with a CD163 specific mAb (2A10 clone), followed by an incubation with Alexa Fluor 594-conjugated goat anti-mouse IgG secondary antibody (red). Cells were counterstained with DAPI (blue).

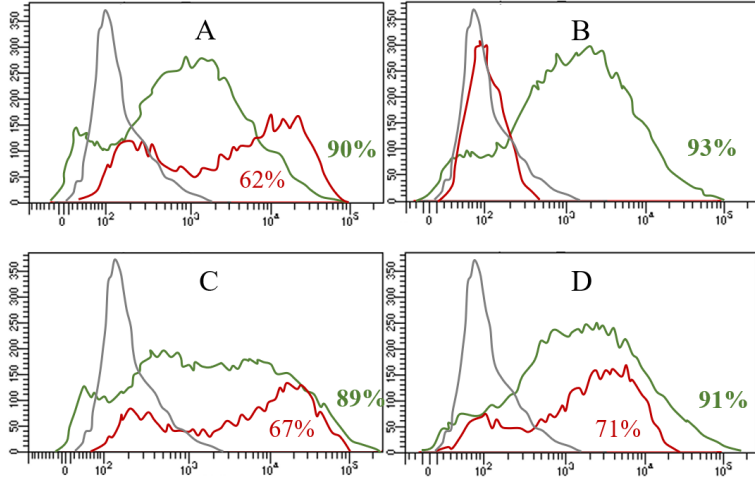


**Figure 4.3. Surface expression of CD163 deletion constructs expressed in HEK cells.** The histograms show the GFP expression green, the mAb 2A10 staining in red and the isotype control in gray. Cells were stained 48 hrs after transfection. The mAb 2A10 staining results are shown as percentage of CD163-positive cells from the GFP-positive gated population.

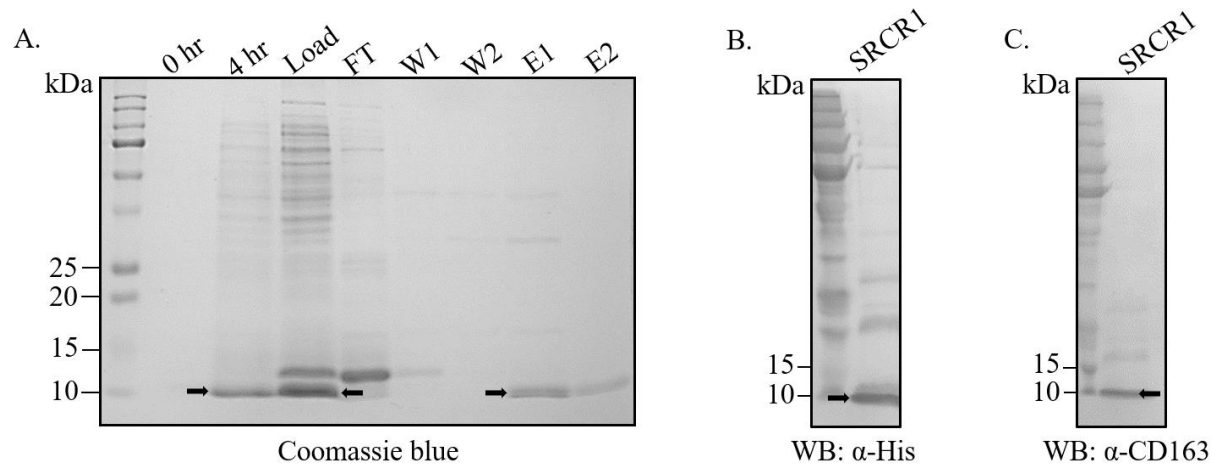


**Figure 4.4. Production of CD163 SRCR1 domain.** (A) SDS-PAGE of His-tagged SRCR1 recombinant protein preparation, followed by Coomassie blue staining. (B) Western blot analysis using anti-His tag mAb. (C) Western blot analysis using anti-CD163 mAb (2A10 clone). For all panels, the left lane shows the molecular weight marker.

## Chapter 5 - Final remarks

Worldwide, porcine reproductive and respiratory syndrome (PRRS) is the most economically challenging infectious disease to ever face the swine industry. As a result of respiratory disease, reproductive failure and reduced weight gain in pigs, PRRS causes more than \$600 million in annual losses to the US industry (Holtkamp et al., 2013). For more than two decades, vaccines have proved to be ineffective in controlling this disease and a new generation of vaccines able to overcome the inability to provide broad cross-protection is most likely still years away.

Recent studies have focused on gene editing as an alternative to cure PRRS. In 2016, Whitworth et al. showed that genetically modified pigs lacking CD163, the PRRSV receptor, fail to support infection by a PRRSV-2 isolate. Since CD163 is involved in different biological processes, such as heme sequestration and modulation of inflammation, the deletion of the entire CD163 protein has important negative consequences. This led to the identification of SRCR5 of CD163 as the key component for PRRSV-1 infection. To demonstrate this, Van Gorp et al. (2010) used an *in vitro* system based on non-permissive HEK293T (HEK) cells transfected with cDNA possessing different CD163 domain deletions and substitution of SRCR5 and the human CD163-like 1 (hCD163L1) protein homolog, SRCR8. However, pigs and macrophages carrying the same domain substitution were resistant to PRRSV-1 infection, but not PRRSV-2.

Therefore, the first goal of this dissertation was to identify the CD163 domain involved in recognition by PRRSV-2. The approach that we used involved the transfection of HEK cells with various domain-deleted CD163 constructs fused to enhanced green fluorescent protein (EGFP) followed by infection with a recombinant PRRSV expressing red fluorescent protein (P129-RFP). This model system identified SRCR5 and Exon 13 region of PSTII as required for

PRRSV-2 infection, similarly to the results reported by Van Gorp (2010). Together, the work done by us and others showed that PRRSV-1 and PRRSV-2 recognize different peptide sequences within SRCR5 of CD163 and that the SRCR4/5 interdomain region, AHRK, might play a role in infection.

The second goal of this dissertation was to evaluate mutations in SRCR5 or SRCR4/5 interdomain region that confer different degrees of permissiveness to PRRSV infection. The approach consisted of preparation of various amino acid mutations within the SRCR4/5 interdomain region along with insertion of proline-arginine (PR) dipeptides along the SRCR5 polyprotein that were probed against infection with PRRSV-1 and PRRSV-2. Based on the rate of infection we identified similarities, but also differences in receptor recognition by the two viruses. Future studies will be directed towards genetically modified pigs with promising CD163 modifications that will be tested for resistance to infection and the capacity of CD163 to retain normal biological function.

The final goal of this dissertation was to identify the location of the epitope recognized by the monoclonal antibody (mAb) 2A10, a commercial antibody widely used in CD163-related studies. The approach used in our experiments was based on the systematic deletion of individual SRCR domains in CD163. As shown by immunofluorescence antibody assay, flow cytometry and western blot, the mAb 2A10 recognizes an epitope within CD163 SRCR1. Future studies will use the same system to further map the exact location of the epitope that this antibody recognizes.

The use of *in vitro* infection models provides comprehensive tools for understanding virus-receptor interactions. The approaches described herein can be used as control strategies for disrupting the interaction between CD163 and specific viral proteins. On a bigger picture, these

various *in vitro* approaches based on the genetic modification of virus receptors on host cells create the means to also understand the role of surface proteins in infection with different other swine diseases.

## **ACKNOWLEDGEMENTS**

We thank Dr. Dongwan Yoo (University of Illinois, College of Veterinary Medicine, USA) who made available the original CD163 construct. This work was supported by the National Pork Board project #16-181 and USDA NIFA award 2016-09462, 2017-2020.

## REFERENCES

- Ansari, I.H.; Kwon, B.; Osorio, F.A.; Pattnaik, A.K. Influence of N-linked glycosylation of porcine reproductive and respiratory syndrome virus GP5 on virus infectivity, antigenicity, and ability to induce neutralizing antibodies. *J. Virol.* **2006**, 80:3994–4004.
- Aruffo, A.; Melnick, M.B.; Linsley, P.S.; Seed, B. The lymphocyte glycoprotein cd6 contains a repeated domain structure characteristic of a new family of cell surface and secreted proteins. *J. Exp. Med.* **1991**, 174:949–952.
- Benfield, D.A.; Nelson, E.; Collins, J.E.; Harris, L.; Goyal, S.M.; Robison, D.; Christianson, W.T.; Morrison, R.B.; Gorcyca, D.; Chladek, D. Characterization of swine infertility and respiratory syndrome (SIRS) virus (Isolate ATCC VR-2332). *J. Vet. Diagnostic Investig.* **1992**, 4:127–133.
- Brinton, M.A.; Godeny, E.K.; Horzinek, M.C.; Meulenberg, J.J.M.; Murtaugh, M.P.; Plagemann, P.G.; Snijder, E.J. Family Arteriviridae. In: van Regenmortel, M.H.V.; Fauquet, C.M.; Bishop, D.H.L.; Carstens, E.B.; Estes, M.K.; Lemon, S.M.; Maniloff, J.; Mayo, M.A.; McGeoch, D.J.; Pringle, C.R.; Wickner, R.B., editors. *Virus Taxonomy—Seventh Report of the International Committee on Taxonomy of Viruses.* *Academic Press* **2000**, 851–857.
- Bullido, R.; Gomez del Moral, M.; Alonso, F.; Ezquerro, A.; Zapata, A.; Sanchez, C.; Ortuno, E.; Alvarez, B.; Dominguez, J. Monoclonal antibodies specific for porcine monocytes/macrophages: macrophage heterogeneity in the pig evidenced by the expression of surface antigens. *Tissue Antigens* **1997**, 49:403–413.
- Burkard, C.; Lillico, S.G.; Reid, E.; Jackson, B.; Mileham, A.J.; Ait-Ali, T.; Whitelaw, C.B.A.; Archibald, A.L. Precision engineering for PRRSV resistance in pigs: Macrophages from genome edited pigs lacking CD163 SRCR5 domain are fully resistant to both PRRSV genotypes while maintaining biological function. *PLoS Pathog.* **2017**, 13(2): e1006206.
- Burkard, C.; Opriessnig, T.; Mileham, A.J.; Stadejek, T.; Ait-Ali, T.; Lillico, S.G.; Whitelaw, C.B.A.; Archibald, A.L. Pigs lacking the scavenger receptor cysteine-rich domain 5 of

- CD163 are resistant to porcine reproductive and respiratory syndrome virus 1 infection. *J. Virol.* **2018**, 92:e00415-18.
- Calvert, J.G.; Slade, D.E.; Shields, S.L.; Jolie, R.; Mannan, R.M.; Ankenbauer, R.G.; Welch, S.-K.W. CD163 expression confers susceptibility to porcine reproductive and respiratory syndrome viruses. *J. Virol.* **2007**, 81:7371–7379.
- Catanzariti, A.-M.; Soboleva, T.A.; Jans, D.A.; Board, P.G.; Baker, R.T. An efficient system for high-level expression and easy purification of authentic recombinant proteins. *Protein Sci.* **2004**, 13:1331–1339.
- Chand, R.J. Study of recombination in Porcine Reproductive and Respiratory Syndrome Virus (PRRSV) using a novel in-vitro system. **2013**, Doctoral Thesis, Kansas State University, Manhattan, KS. Retrieved from <https://krex.k-state.edu/dspace/bitstream/handle/2097/16926/RanjniChand2013.pdf?sequence=3>.
- Chen, W.; Cui, J.; Wang, J.; Sun, Y.; Ji, C.; Song, R.; Zeng, Y.; Pan, H.; Sheng, J.; Zhang, G.; et al. Phages bearing specific peptides with affinity for porcine reproductive and respiratory syndrome virus GP4 protein prevent cell penetration of the virus. *Vet. Microbiol.* **2018**, 224:43–49.
- Collins, J.E.; Benfield, D.A.; Christianson, W.T.; Harris, L.; Hennings, J.C.; Shaw, D.P.; Goyal, S.M.; McCullough, S.; Morrison, R.B.; Joo, H.S.; et al. Isolation of swine infertility and respiratory syndrome virus (Isolate ATCC VR-2332) in North America and experimental reproduction of the disease in gnotobiotic pigs. *J. Vet. Diagnostic Investig.* **1992**, 4:117–126.
- Costers, S.; Lefebvre, D.J.; Van Doorselaere, J.; Vanhee, M.; Delputte, P.L.; Nauwynck, H.J. GP4 of porcine reproductive and respiratory syndrome virus contains a neutralizing epitope that is susceptible to immunoselection in vitro. *Arch. Virol.* **2010**, 155:371–378.
- Das, P.B.; Dinh, P.X.; Ansari, I.H.; de Lima, M.; Osorio, F.A.; Pattnaik, A.K. The minor envelope glycoproteins GP2a and GP4 of porcine reproductive and respiratory syndrome virus interact with the receptor CD163. *J. Virol.* **2010**, 84:1731–1740.

- Das, P.B.; Vu, H.L.X.; Dinh, P.X.; Cooney, J.L.; Kwon, B.; Osorio, F.A.; Pattnaik, A.K. Glycosylation of minor envelope glycoproteins of porcine reproductive and respiratory syndrome virus in infectious virus recovery, receptor interaction, and immune response. *Virology* **2011**, 410:385–394.
- DeLano, W.L. References. *Hypertens. Res.* **2014**, 37:362–387.
- Delisle, B.; Gagnon, C.A.; Lambert, M.-È.; D’Allaire, S. Porcine reproductive and respiratory syndrome virus diversity of Eastern Canada swine herds in a large sequence dataset reveals two hypervariable regions under positive selection. *Infect. Genet. Evol.* **2012**, 12:1111–1119.
- Delputte, P.L.; Vanderheijden, N.; Nauwynck, H.J.; Pensaert, M.B. Involvement of the matrix protein in attachment of porcine reproductive and respiratory syndrome virus to a heparinlike receptor on porcine alveolar macrophages. *J. Virol.* **2002**, 76:4312–4320.
- Du, Y.; Pattnaik, A.K.; Song, C.; Yoo, D.; Li G. Glycosyl-phosphatidylinositol (GPI)-anchored membrane association of the porcine reproductive and respiratory syndrome virus GP4 glycoprotein and its co-localization with CD163 in lipid rafts. *Virology.* **2012**, 424:18–32.
- Duan, X.; Nauwynck, H.J.; Pensaert, M.B. Virus quantification and identification of cellular targets in the lungs and lymphoid tissues of pigs at different time intervals after inoculation with porcine reproductive and respiratory syndrome virus (PRRSV). *Vet. Microbiol.* **1997**, 56:9–19.
- Faaberg, K.S.; Hocker, J.D.; Erdman, M.M.; Harris, D.L.H.; Nelson, E.A.; Torremorell, M.; Plagemann, P.G.W. Neutralizing antibody responses of pigs infected with natural GP5 N-glycan mutants of porcine reproductive and respiratory syndrome virus. *Viral Immunol.* **2006**, 19:294–304.
- Fabriek, B.O.; Dijkstra, C.D.; van den Berg, T.K. The macrophage scavenger receptor CD163. *Immunobiology* **2005**, 210:153–160.
- Fabriek, B.O.; Polfliet, M.M.J.; Vloet, R.P.M.; van der Schors, R.C.; Ligtenberg, A.J.M.; Weaver, L.K.; Geest, C.; Matsuno, K.; Moestrup, S.K.; Dijkstra, C.D.; et al. The

- macrophage CD163 surface glycoprotein is an erythroblast adhesion receptor. *Blood* **2007**, 109:5223–5229.
- Fabriek, B.O.; van Bruggen, R.; Deng, D.M.; Ligtenberg, A.J.M.; Nazmi, K.; Schornagel, K.; Vloet, R.P.M.; Dijkstra, C.D.; van den Berg, T.K. The macrophage scavenger receptor CD163 functions as an innate immune sensor for bacteria. *Blood* **2009**, 113:887–892.
- Graversen, J.H.; Madsen, M.; Moestrup, S.K. CD163: a signal receptor scavenging haptoglobin–hemoglobin complexes from plasma. *Int. J. Biochem. Cell Biol.* **2002**, 34:309–314.
- Gulyaeva, A.A.; Lauber, C.; Samborskiy, D.V.; Leontovich, A.M.; Sidorov, I.A.; Gorbalenya, A.E. Evolutionary based classification of genomic diversity of nidoviruses connects metagenomics and experimental research; Proceedings of the 14th International Nidovirus Symposium; Kansas City, MO, USA. 4–9 June **2017**.
- Guo, C.; Wang, M.; Zhu, Z.; He, S.; Liu, H.; Liu, X.; Shi, X.; Tang, T.; Yu, P.; Zeng, J.; et al. Highly efficient generation of pigs harboring a partial deletion of the CD163 SRCR5 domain, which are fully resistant to porcine reproductive and respiratory syndrome virus 2 infection. *Front. Immunol.* **2019**, 10:1846.
- Holtkamp, D. J.; Kliebenstein, J. B.; Neumann, E. J.; Zimmerman, J. J.; Rotto, H. F.; Yoder, T. K.; et al. Assessment of the economic impact of porcine reproductive and respiratory syndrome virus on United States pork producers. *J. Swine Health Prod.* **2013**, 21:72–84.
- Johnson, C.R.; Griggs, T.F.; Gnanandarajah, J.; Murtaugh, M.P. Novel structural protein in porcine reproductive and respiratory syndrome virus encoded by an alternative ORF5 present in all arteriviruses. *J. Gen. Virol.* **2011**, 92:1107–1116.
- Kappes, M.A.; Miller, C.L.; Faaberg, K.S. Highly divergent strains of porcine reproductive and respiratory syndrome virus incorporate multiple isoforms of nonstructural protein 2 into virions. *J. Virol.* **2013**, 87:13456–13465.
- Keffaber, K.K. Reproductive failure of unknown etiology. *Am. Assoc. Swine Pr. News* **1989**, 2: 1–9.

- Kimpston-Burkgren, K.; Correias, I.; Osorio, F.A.; Steffen, D.; Pattnaik, A.K.; Fang, Y.; Vu, H.L.X. Relative contribution of porcine reproductive and respiratory syndrome virus open reading frames 2–4 to the induction of protective immunity. *Vaccine* **2017**, *35*:4408–4413.
- Kristiansen, M.; Graversen, J.H.; Jacobsen, C.; Sonne, O.; Hoffman, H.-J.; Law, S.K.A.; Moestrup, S.K. Identification of the haemoglobin scavenger receptor. *Nature* **2001**, *409*:198–201.
- Kuhn, J.H.; Lauck, M.; Bailey, A.L.; Shchetinin, A.M.; Vishnevskaya, T. V.; Bào, Y.; Ng, T.F.F.; LeBreton, M.; Schneider, B.S.; Gillis, A.; et al. Reorganization and expansion of the nidoviral family Arteriviridae. *Arch. Virol.* **2016**, *161*: 755–768.
- Ligtenberg, A.J.M.; Veerman, E.C.I.; Nieuw Amerongen, A. V.; Mollenhauer, J. Salivary agglutinin/glycoprotein-340/DMBT1: A single molecule with variable composition and with different functions in infection, inflammation and cancer. *Biol. Chem.* **2007**, *388*:1275-1289.
- Ma, H.; Jiang, L.; Qiao, S.; Zhi, Y.; Chen, X.-X.; Yang, Y.; Huang, X.; Huang, M.; Li, R.; Zhang, G.-P. The crystal structure of the fifth scavenger receptor cysteine-rich domain of porcine CD163 reveals an important residue involved in porcine reproductive and respiratory syndrome virus infection. *J. Virol.* **2017**, *91*.
- Matanin, B.M.; Huang, Y.; Meng, X.J.; Zhang, C. Purification of the major envelop protein GP5 of porcine reproductive and respiratory syndrome virus (PRRSV) from native virions. *J. Virol. Methods* **2008**, *147*:127–135.
- Meulenbergh, J.J.; van Nieuwstadt, A.P.; van Essen-Zandbergen, A.; Langeveld, J.P. Posttranslational processing and identification of a neutralization domain of the GP4 protein encoded by ORF4 of Lelystad virus. *J. Virol.* **1997**, *71*:6061–6067.
- Nielsen, M.J. The macrophage scavenger receptor CD163: endocytic properties of cytoplasmic tail variants. *J. Leukoc. Biol.* **2006**, *79*:837–845.

- Oleksiewicz, M.B.; Botner, A.; Toft, P.; Normann, P.; Storgaard, T. Epitope mapping porcine reproductive and respiratory syndrome virus by phage display: the nsp2 fragment of the replicase polyprotein contains a cluster of B-cell epitopes. *J. Virol.* **2001**, *75*:3277–3290.
- Ostrowski, M.; Galeota, J.A.; Jar, A.M.; Platt, K.B.; Osorio, F.A.; Lopez, O.J. Identification of neutralizing and nonneutralizing epitopes in the porcine reproductive and respiratory syndrome virus GP5 ectodomain. *J. Virol.* **2002**, *76*:4241–4250.
- Pei, Y.; Hodgins, D.C.; Wu, J.; Welch, S.-K.W.; Calvert, J.G.; Li, G.; Du, Y.; Song, C.; Yoo, D. Porcine reproductive and respiratory syndrome virus as a vector: Immunogenicity of green fluorescent protein and porcine circovirus type 2 capsid expressed from dedicated subgenomic RNAs. *Virology* **2009**, 389:91–99.
- Pettersen, E.F.; Goddard, T.D.; Huang, C.C.; Couch, G.S.; Greenblatt, D.M.; Meng, E.C.; Ferrin, T.E. UCSF Chimera? A visualization system for exploratory research and analysis. *J. Comput. Chem.* **2004**, *25*:1605–1612.
- Plagemann, P.G.W. Complexity of the single linear neutralization epitope of the mouse arterivirus lactate dehydrogenase-elevating virus. *Virology* **2001**, 290:11–20.
- Plagemann, P.G.W.; Rowland, R.R.R.; Faaberg, K.S. The primary neutralization epitope of porcine respiratory and reproductive syndrome virus strain VR-2332 is located in the middle of the GP5 ectodomain. *Arch. Virol.* **2002**, *147*:2327–2347.
- Plagemann, P.G.W. Porcine reproductive and respiratory syndrome virus: Origin hypothesis. *Emerg. Infect. Dis.* **2003**, *9*:903–908.
- Plagemann, P.G.W. The primary GP5 neutralization epitope of North American isolates of porcine reproductive and respiratory syndrome virus. *Vet. Immunol. Immunopathol.* **2004**, *102*:263–275.
- Popescu, L.N.; Tribble, B.R.; Chen, N.; Rowland, R.R.R. GP5 of porcine reproductive and respiratory syndrome virus (PRRSV) as a target for homologous and broadly neutralizing antibodies. *Vet. Microbiol.* **2017**, *209*:90–96.

- Prather, R.S.; Rowland, R.R.R.; Ewen, C.; Tribble, B.; Kerrigan, M.; Bawa, B.; Teson, J.M.; Mao, J.; Lee, K.; Samuel, M.S.; et al. An intact sialoadhesin (Sn/SIGLEC1/CD169) is not required for attachment/internalization of the porcine reproductive and respiratory syndrome virus. *J. Virol.* **2013**, *87*:9538–9546.
- Reed, J.L.; Muench, H. A simple method of estimating fifty percent endpoints. *Am. J. Epidemiol.* **1938**, *27*:493–497.
- Ritter, M.; Buechler, C.; Langmann, T.; Schmitz, G. Genomic organization and chromosomal localization of the human CD163 (M130) gene: A member of the scavenger receptor cysteine-rich superfamily. *Biochem. Biophys. Res. Commun.* **1999**, *260*:466–474.
- Robinson, S.R.; Li, J.; Nelson, E.A.; Murtaugh, M.P. Broadly neutralizing antibodies against the rapidly evolving porcine reproductive and respiratory syndrome virus. *Virus Res.* **2015**, *203*:56–65.
- Sánchez, C.; Doménech, N.; Alonso, F.; Ezquerro, A.; Domínguez, J.; Vázquez, J. The porcine 2A10 antigen is homologous to human CD163 and related to macrophage differentiation. *J. Immunol.* **1999**, *162*:5230–5237.
- Sarrias, M.R.; Gronlund, J.; Padilla, O.; Madsen, J.; Holmskov, U.; Lozano, F. The scavenger receptor cysteine-rich (SRCR) domain: an ancient and highly conserved protein module of the innate immune system. *Crit. Rev. Immunol.* **2004**, *24*:1–38.
- Soares, M.P.; Bach, F.H. Heme oxygenase-1: from biology to therapeutic potential. *Trends Mol. Med.* **2009**, *15*:50–58.
- Spilman, M.S.; Welbon, C.; Nelson, E.; Dokland, T. Cryo-electron tomography of porcine reproductive and respiratory syndrome virus: organization of the nucleocapsid. *J. Gen. Virol.* **2009**, *90*:527–535.
- Stoian, A.M.M.; Rowland, R.R.R. Challenges for porcine reproductive and respiratory syndrome (PRRS) vaccine design: Reviewing virus glycoprotein interactions with CD163 and targets of virus neutralization. *Vet. Sci.* **2019**, *6*:9.

- Teifke, J.P.; Dauber, M.; Fichtner, D.; Lenk, M.; Polster, U.; Weiland, E.; Beyer, J. Detection of European porcine reproductive and respiratory syndrome virus in porcine alveolar macrophages by two-colour immunofluorescence and in-situ hybridization-immunohistochemistry double labelling. *J. Comp. Pathol.* **2001**, 124:238–245.
- Trible, B.R.; Popescu, L.N.; Monday, N.; Calvert, J.G.; Rowland, R.R.R. A single amino acid deletion in the matrix protein of porcine reproductive and respiratory syndrome virus confers resistance to a polyclonal swine antibody with broadly neutralizing activity. *J. Virol.* **2015**, 89:6515–6520.
- Van Breedam, W.; Van Gorp, H.; Zhang, J.Q.; Crocker, P.R.; Delputte, P.L.; Nauwynck, H.J. The M/GP5 glycoprotein complex of porcine reproductive and respiratory syndrome virus binds the sialoadhesin receptor in a sialic acid-dependent manner. *PLoS Pathog.* **2010**, 6:e1000730.
- Van Gorp, H.; Van Breedam, W.; Delputte, P.L.; Nauwynck, H.J. Sialoadhesin and CD163 join forces during entry of the porcine reproductive and respiratory syndrome virus. *J. Gen. Virol.* **2008**, 89:2943–2953.
- Van Gorp, H.; Van Breedam, W.; Delputte, P.L.; Nauwynck, H.J. The porcine reproductive and respiratory syndrome virus requires trafficking through CD163-positive early endosomes, but not late endosomes, for productive infection. *Arch. Virol.* **2009**, 154:1939–1943.
- Van Gorp, H.; Delputte, P.L.; Nauwynck, H.J. Scavenger receptor CD163, a Jack-of-all-trades and potential target for cell-directed therapy. *Mol. Immunol.* **2010**, 47:1650–1660.
- Van Gorp, H.; Van Breedam, W.; Van Doorselaere, J.; Delputte, P.L.; Nauwynck, H.J. Identification of the CD163 protein domains involved in infection of the porcine reproductive and respiratory syndrome virus. *J. Virol.* **2010**, 84:3101–3105.
- Vanderheijden, N.; Delputte, P.L.; Favoreel, H.W.; Vandekerckhove, J.; Van Damme, J.; van Woensel, P.A.; Nauwynck, H.J. Involvement of sialoadhesin in entry of porcine reproductive and respiratory syndrome virus into porcine alveolar macrophages. *J. Virol.* **2003**, 77:8207–8215.

- Vanhee, M.; Costers, S.; Van Breedam, W.; Geldhof, M.F.; Van Doorselaere, J.; Nauwynck, H.J. A variable region in GP4 of European-type porcine reproductive and respiratory syndrome virus induces neutralizing antibodies against homologous but not heterologous virus strains. *Viral Immunol.* **2010**, *23*:403–413.
- Vanhee, M.; Van Breedam, W.; Costers, S.; Geldhof, M.; Noppe, Y.; Nauwynck, H. Characterization of antigenic regions in the porcine reproductive and respiratory syndrome virus by the use of peptide-specific serum antibodies. *Vaccine* **2011**, *29*:4794–4804.
- Vu, H.L.X.; Kwon, B.; Yoon, K.-J.; Laegreid, W.W.; Pattnaik, A.K.; Osorio, F.A. Immune evasion of porcine reproductive and respiratory syndrome virus through glycan shielding involves both glycoprotein 5 as well as glycoprotein 3. *J. Virol.* **2011**, *85*:5555–5564.
- Welch, S.K.W.; Calvert, J.G. A brief review of CD163 and its role in PRRSV infection. *Virus Res.* **2010**, *154*:98–103.
- Wells, K.D.; Bardot, R.; Whitworth, K.M.; Tribble, B.R.; Fang, Y.; Mileham, A.; Kerrigan, M.A.; Samuel, M.S.; Prather, R.S.; Rowland, R.R.R. Replacement of porcine CD163 scavenger receptor cysteine-rich domain 5 with a CD163-like homolog confers resistance of pigs to genotype 1 but not genotype 2 porcine reproductive and respiratory syndrome virus. *J. Virol.* **2017**, *91*:2-11.
- Wensvoort, G.; Terpstra, C.; Pol, J.M.A.; ter Laak, E.A.; Bloemraad, M.; de Kluyver, E.P.; Kragten, C.; van Buiten, L.; den Besten, A.; Wagenaar, F.; et al. Mystery swine disease in the Netherlands: The isolation of Lelystad virus. *Vet. Q.* **1991**, *13*:121–130.
- Whitworth, K.M.; Rowland, R.R.R.; Ewen, C.L.; Tribble, B.R.; Kerrigan, M.A.; Cino-Ozuna, A.G.; Samuel, M.S.; McLaren, D.; Mileham, A.; Wells, K.D.; Prather, R.S. CD163 facilitates both entry and replication of porcine reproductive and respiratory syndrome virus. *Nature Biotech.* **2016**, *34*:20-22.

- Wu, W.-H.; Fang, Y.; Farwell, R.; Steffen-Bien, M.; Rowland, R.R.R.; Christopher-Hennings, J.; Nelson, E.A. A 10-kDa structural protein of porcine reproductive and respiratory syndrome virus encoded by ORF2b. *Virology* **2001**, 287:183–191.
- Xie, J.; Christiaens, I.; Yang, B.; Trus, I.; Devriendt, B.; Cui, T.; Wei, R.; Nauwynck, H.J. Preferential use of Siglec-1 or Siglec-10 by type 1 and type 2 PRRSV strains to infect PK15S1–CD163 and PK15S10–CD163 cells. *Vet. Res.* **2018**, 49:1–13.
- Yang, J.; Yan, R.; Roy, A.; Xu, D.; Poisson, J.; Zhang, Y. The I-TASSER Suite: protein structure and function prediction. *Nat. Methods* **2015**, 12:7–8.
- Yu, P.; Wei, R.; Dong, W.; Zhu, Z.; Zhang, X.; Chen, Y.; Liu, X.; Guo, C. CD163 $\Delta$ SRCR5 MARC-145 cells resist PRRSV-2 infection via inhibiting virus uncoating, which requires the interaction of CD163 with Calpain 1. *Front. Microbiol.* **2020**, 10:3115.
- Zhou, Y.-J.; An, T.-Q.; He, Y.-X.; Liu, J.-X.; Qiu, H.-J.; Wang, Y.-F.; Tong, G. Antigenic structure analysis of glycosylated protein 3 of porcine reproductive and respiratory syndrome virus. *Virus Res.* **2006**, 118:98–104.